

Review

Multifunctional magnetic iron oxide nanoparticles: an advanced platform for cancer theranostics

Shengzhe Zhao^{1,2,3,#}, Xujiang Yu^{3,#}, Yuna Qian², Wei Chen^{1,✉}, Jianliang Shen^{1,2,✉}

1. State Key Laboratory of Ophthalmology, Optometry and Vision Science, School of Ophthalmology & Optometry, School of Biomedical Engineering, Wenzhou Medical University, Wenzhou 325027, China
2. Wenzhou Institute, University of Chinese Academy of Sciences, Wenzhou 32500, China.
3. State Key Lab of Metal Matrix Composites, School of Chemistry and Chemical Engineering, Shanghai Jiao Tong University, Shanghai 200240, China.

#These authors contributed equally to this work.

✉ Corresponding authors: Jianliang Shen (shenjl@wibe.ac.cn) or Wei Chen (chenweimd@hotmail.com)

© The author(s). This is an open access article distributed under the terms of the Creative Commons Attribution License (<https://creativecommons.org/licenses/by/4.0/>). See <http://ivyspring.com/terms> for full terms and conditions.

Received: 2019.11.29; Accepted: 2020.04.27; Published: 2020.05.15

Abstract

Multifunctional magnetic nanoparticles and derivative nanocomposites have aroused great concern for multimode imaging and cancer synergistic therapies in recent years. Among the rest, functional magnetic iron oxide nanoparticles (Fe_3O_4 NPs) have shown great potential as an advanced platform because of their inherent magnetic resonance imaging (MRI), biocatalytic activity (nanozyme), magnetic hyperthermia treatment (MHT), photo-responsive therapy and drug delivery for chemotherapy and gene therapy. Magnetic Fe_3O_4 NPs can be synthesized through several methods and easily surface modified with biocompatible materials or active targeting moieties. The MRI capacity could be appropriately modulated to induce response between T_1 and T_2 modes by controlling the size distribution of Fe_3O_4 NPs. Besides, small-size nanoparticles are also desired due to the enhanced permeation and retention (EPR) effect, thus the imaging and therapeutic efficiency of Fe_3O_4 NP-based platforms can be further improved. Here, we firstly retrospect the typical synthesis and surface modification methods of magnetic Fe_3O_4 NPs. Then, the latest biomedical application including responsive MRI, multimodal imaging, nanozyme, MHT, photo-responsive therapy and drug delivery, the mechanism of corresponding treatments and cooperation therapeutics of multifunctional Fe_3O_4 NPs are also be explained. Finally, we also outline a brief discussion and perspective on the possibility of further clinical translations of these multifunctional nanomaterials. This review would provide a comprehensive reference for readers to understand the multifunctional Fe_3O_4 NPs in cancer diagnosis and treatment.

Key words: magnetic iron oxide nanoparticles, multifunctional nanoplatform, multimodal imaging, drug delivery, cancer diagnosis and treatment

Introduction

Cancer is a class of diseases marked by the malignant proliferation of tumor cells. Despite of the huge advancements achieved during the past decades, cancer still a serious public health issue, which leading the main deaths around the world every year [1]. With the development of nanotechnology, multifunctional nanoparticle-based systems have been emerged as a new approach for efficient cancer diagnosis and treatment due to their inherent advantages in overcoming the deficiencies compared to the traditional cancer diagnostic and

therapeutic techniques, such as low efficacy, drug resistance or other side effects [2-5]. Currently, various multifunctional nanoparticle-based systems integrating nanotechnology and molecular biology together have been developed as powerful tools for cancer early-stage diagnosis, real-time imaging and precise therapy [6-10]. The integration of single functional component within a multifunctional therapeutic system has been demonstrated as one effective treatment approach for fighting the cancer [11-13]. The ideal nanoparticle-based diagnosis and

treatment systems should not only contain the unique physical, chemical and medical properties of nanoparticles, but also be smart carriers to effectively deliver anticancer agents, thus realizing multi-modal imaging and combined therapeutic effects [14-17]. Moreover, the diverse nanostructures and surface modification of nanomaterials should endow themselves with the tumor-targeting ability by EPR effect or other interactions affiliated to the features of tumor tissues [18-21].

Magnetic iron oxide nanoparticles (Fe_3O_4 NPs) are one representative candidate of multifunctional nanomaterials with increasing utilization in many biomedical fields, including magnetic resonance imaging (MRI), biological catalysis, magnetic hyperthermia, magnetic targeting, magnetic separation, photo-responsive therapy and drug-delivery, and currently have been widely used in tumor diagnosis and treatment [22-28]. Meanwhile, according to the specific treatment demand and characteristics of the tumor microenvironment, decoration of the Fe_3O_4 NPs with different functionalization factors can form the multifunctional iron oxide nanoparticles to achieve better therapeutic effects [29-31]. Compared to other imaging modalities in clinic, MRI exhibits high spatial resolution with rapid *in vivo* image acquisition [32, 33]. To improve its sensitivity, MRI contrast agents are usually used, which can be divided into two types, namely T_1 and T_2 agents depending on their unique effects to alter the longitudinal or transverse relaxation time of water protons [34-36]. Compared to the widely used T_1 -weighted MRI agents of gadolinium (Gd)-based contrast agents with shortcoming of unpredictable renal toxicity and blood circulation time, Fe_3O_4 NPs are contrast agents that can be used for either T_1 or T_2 -weighted imaging with better biosecurity [13, 37-39]. In particular, Fe_3O_4 NPs is a typical T_2 contrast agent, when the size of Fe_3O_4 less than 5 nm, the decreased magnetic moment will strongly suppressed T_2 effect, thus they can also be used for T_1 -weighted MRI imaging, which provides a possibility to prepare responsive T_2-T_1 switching MRI contrast agents [40, 41]. Due to the excellent thermal effect under the oscillating magnetic field, magnetic Fe_3O_4 NPs are widely used in the field of magnetic hyperthermia treatment of tumors [42]. Besides, Fe_3O_4 NPs also show catalytic activity analogous peroxidase and considered as mimic enzyme for cancer therapy through the well-known Fenton reactions, which could catalyst endogenous hydrogen peroxide (H_2O_2) into the hydroxyl radical ($\cdot\text{OH}$) with high cytotoxicity and cause the death of tumor cells [43, 44]. This newly defined chemodynamic therapy (CDT) based on the Fenton reaction is a rapidly developing research topic

in cancer treatment these years and have endowed magnetic Fe_3O_4 NPs with a brand-new life [45].

The modification of functional components onto Fe_3O_4 NPs can also bring photo-responsive therapy, namely photothermal therapy or photodynamic therapy, and makes Fe_3O_4 NPs functionalize as advanced nanoplatforms for oncotherapy [46]. For example, the modification of magnetic Fe_3O_4 NPs with the classic photothermal treatment agent of Au NPs can bring additional photothermal therapeutic capability besides to the MRI and magnetic targeting functionality, thus improving the accuracy of diagnosis and treatment of tumor using Fe_3O_4 NPs [47]. Similar, Fe_3O_4 NPs also have other advantages, such as prolonged blood circulation, fast clearance, low side-effects, excellent imaging and therapeutic efficiency. Therefore, several types of magnetic Fe_3O_4 -based NPs systems have been approved to translate from experimental stages to clinical applications by the food and drug administration (FDA), some of them have reached the market for clinic (Table 1) [48, 49]. For example, the contrast agent AMI-25 (Ferumoxide, Feridex IV, Endorem) consists of the dextran coated Fe_3O_4 nanocrystal has been used in clinic, this agent could rapidly agglomeration in liver and spleen after injection 1 h, and the optimal imaging effects will appear in liver and spleen after injection 2 h and 4 h, respectively.

To improve the efficacy of Fe_3O_4 NPs in tumor imaging and therapeutic, as well as other inorganic nanomaterials, a maximum tumor accumulation is highly desired [50, 51]. Besides to the passive EPR effect [52, 53], the more positive method to increase tumor accumulation of nanomaterials is to conjugation tumor-homing or tumor microenvironment (TME) responsive ligands onto the Fe_3O_4 NPs to purposively improve their final amount in tumor tissues through the selective recognition and internalization by tumor cells [54-57]. Synthesized Fe_3O_4 NPs through common chemical methods are usually coated with the hydrophobic alkyl ligands on the outer surface. Surface modification and further functionalization are necessary to convert them into hydrophilic, improve their biocompatibility and blood circulation time for enhancing tumor accumulation [13, 58], which are also beneficial to reduce the unexpected damage to normal tissues.

Smart drug-delivery systems based on nanoparticles is another vital way to combine chemotherapy with nanotheranostics [59, 60]. Fe_3O_4 NPs can easily be functionalized into a multifunctional platform by modifying with various therapeutic agents, and the common functional components for surface modification can be classified as: (1) small molecule (e.g., carboxylates, oleic acid)

[61, 62]; (2) biomolecules (nucleic acids (siRNA), peptides and proteins) [63-65]; (3) inorganic materials (e.g., Au, Ag, MoS₂) [25, 66, 67]; (4) mesoporous materials (e.g., mesoporous silica, metal-organic frameworks) [68, 69]; (5) polymers (e.g., polyvinylpyrrolidone (PVP), polyethylene glycol (PEG), polyethyleneimine (PEI)) [70-72]. Surface modification with these components of nanoparticles usually have a low cytotoxicity, hydrophilic, large pore volume, high surface area, adjustable pore size, in consequence provides the nanoparticles with better biocompatible and biodegradable [73, 74]. Based on these, through surface modification and functionalization increases the ability of Fe₃O₄ NPs in tumor targeting and responsiveness that further enhance their therapeutic effect [75].

This review aims to summarize the recent progress to provide a clear explanation for the rational design, construction and applications of Fe₃O₄ NPs-based multifunctional platform. Firstly, we introduce the common synthesis methods. Secondly, the surface modification and targeting ligand conjugation of Fe₃O₄ NPs are described. Finally, we will focus on the recent development of multifunctional Fe₃O₄ platforms for cancer diagnosis and treatment, including responsive imaging, nanzyme, CDT, magnetic hyperthermia (MHT), photothermal therapy (PTT), photodynamic therapy

(PDT) and drug/gene delivery. We believe the summary of recent development will provide a comprehensive understanding of the applications of Fe₃O₄-based NPs multifunctional systems in biomedical research studies and clinic uses.

Synthesis of magnetic Fe₃O₄ NPs

The properties of magnetic Fe₃O₄ NPs are initially determined by their size and morphology. Thus, the selection of suitable synthesis method is important. Fe₃O₄ NPs can be synthesized by physical, biosynthetic and chemical methods [76-78]. Generally, the physical synthesis methods, mainly including the ball grinding method, electron beam lithography, aerosol and gas phase deposition, fail to regulate the size into the nanoscale [79-81]. Biosynthetic methods to synthesize magnetic nanoparticles is an emerging technology, which generates magnetosomes through the regulation of biological macromolecules and iron element by magnetotactic bacteria or cells [82, 83]. However, these methods are always accompanied with the disadvantages of long synthesis time, low yield and broad size distributions. In comparison, the chemical synthesis methods are relatively common because of the advantages of simple operation, low cost and huge production yields. Therefore, we will only focus on the chemical methods in the main text.

Table 1. Applications of magnetic Fe₃O₄ NPs in clinic.

Name	Short name	Size (nm)	Coating	Blood half in patients	r_1 (mmol ⁻¹ s ⁻¹)	r_2 (mmol ⁻¹ s ⁻¹)	Type of contrast	Clinical dose	Application
Ferumoxide	AMI-25	120-180	Dextran	10 min	24	100-160	Negative	30 μmol Fe/kg	Liver/spleen I imaging
Ferumoxytol	AMI-7228	3	Carboxymethyl-dextran	14 h	15	89	Positive	50-400 μmol Fe/kg	Angiography IV
Ferumoxsil	AMI-121	300	Silica	Not available	3	72	Negative	105 mg/patient	GI oral imaging
Ferumoxtran	AMI-227	30	Dextran	24-30 h	22	44-85	Positive/Negative	45 μmol Fe/kg	Lymph node bone imaging
Feruglose	NC1001 50	10-20	Carbohydrate polyethylene glycol	2h	20	35	Positive	36 μmol Fe/kg	Perfusion angiography
Ferucarbotran SHU-555A	SHU-555A	60-80	Carboxydextrans	12 min	25	164-177	Negative	8-12 μmol Fe/kg	Liver/spleen IV imaging
Ferucarbotran SHU-555C	SHU-555C	20-50	Carboxydextrans	6-8 h	7	57	Positive	40 μmol Fe/kg	Perfusion lymph node bone marrow IV

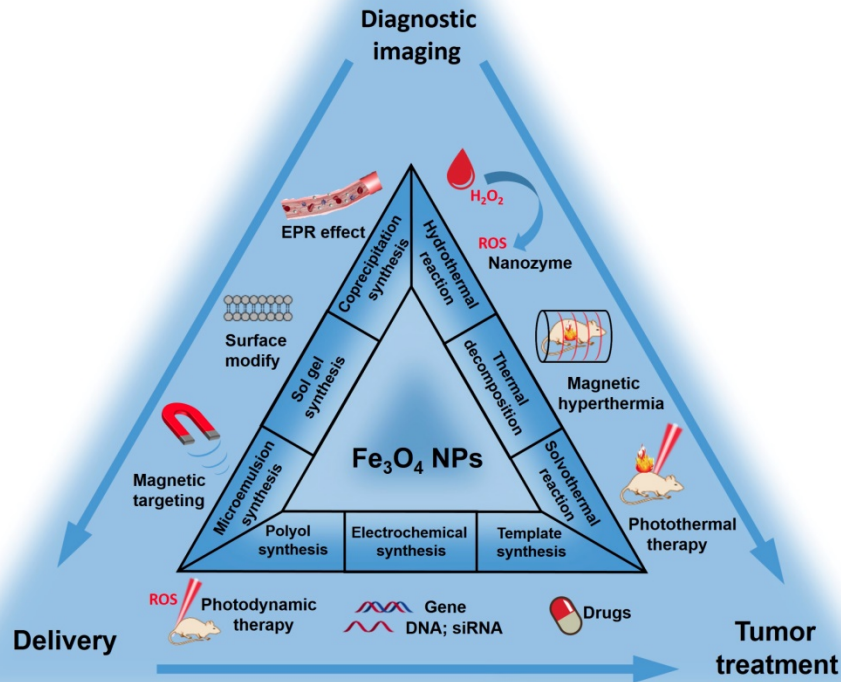


Figure 1. Typical synthesis methods of magnetic Fe_3O_4 NPs and their applications in cancer diagnosis and treatment.

In general, the key to synthesize monodisperse Fe_3O_4 NPs in solution is to control the processes of nucleation and growth [84, 85]. Different synthetic strategies produce Fe_3O_4 NPs usual with different morphology, sizes, crystallinity and surface properties [86, 87]. The common chemical synthesis methods include thermal decomposition [88, 89], solvothermal reaction [90], polyol synthesis [91], hydrothermal reaction [92], coprecipitation synthesis [93, 94], microemulsion synthesis [95], sol-gel synthesis [96], and template synthesis [97] (Figure 1). Here we will detailly introduce the recent advances using the above methods for the synthesis of Fe_3O_4 NPs (Table 2).

Thermal decomposition

Thermal decomposition of organometallic precursors into metal oxides or metal elements at high temperature is a classic method to synthesize monodisperse nanocrystals [79, 88, 89]. Due to the presence of organic ligands, the aggregation and overgrowth of nanoparticles are restricted and the diameter of nanoparticles is closely related to the reaction time and the boiling point of organic solvent [98]. Generally, the metal complex precursors are rapidly injected into hot organic solvents or directly heated up with the solvents [99, 100]. In the hot injection process, after the metal precursors solution is

rapidly injected into the solvents at the reaction temperature, an instant nucleation immediately happens with a controlled growth process. In the heating-up procedure, the nucleation increases gradually with the raise of the reaction temperatures [101-103]. Oleic acid (OA), oleylamine (OAm) and 1-octadecene (ODE) are the commonly used solvents as well as surfactants to stabilize nanoparticles and control their sizes and morphologies [104]. It is worth mentioning that the surface of nanoparticles prepared by this method is hydrophobic, and subsequent surface modification is needed to improve the hydrophilicity for the utilization in biological environment [105]. Hyeon *et al.* first prepared uniform and small-sized monodisperse Fe_3O_4 nanocrystals (4-12 nm) through this method [88, 89]. The size of the Fe_3O_4 nanocrystals were controlled by the boiling points (b.p.) of the organic solvent. As shown in Figure 2A, the size of Fe_3O_4 nanocrystals increases with the rise of solvent boiling point. This method has been widely used for synthesis uniform small-size Fe_3O_4 NPs with good crystallinity and be widely used in the application of MRI contrast agent, drug carrier, further assembly forms cluster structure use for photothermal or magnetic hyperthermia treatment of tumors, which shows great significance to the biological application of Fe_3O_4 .

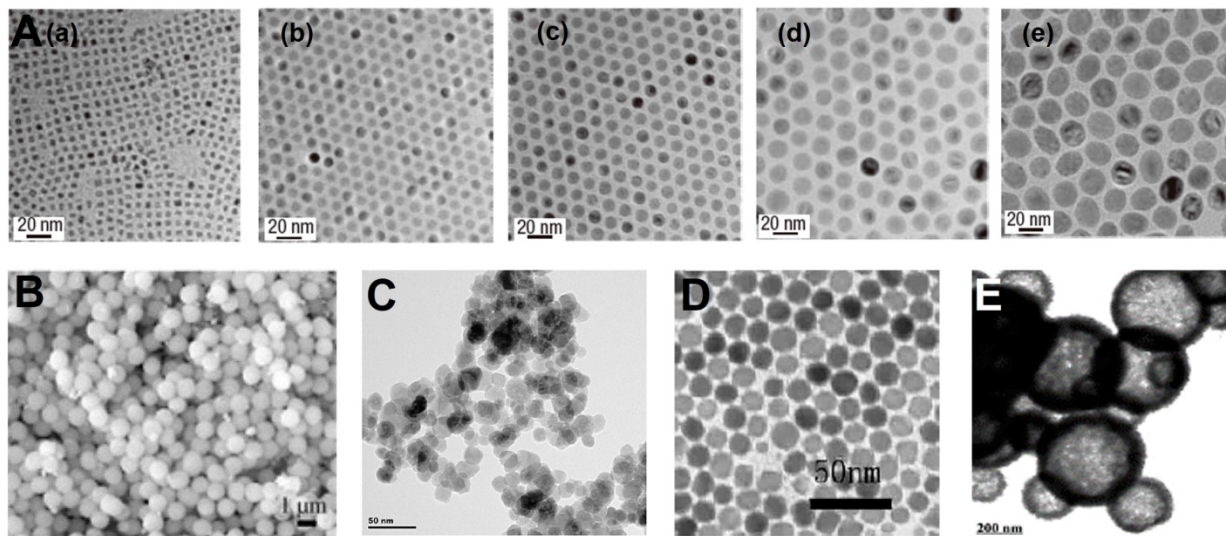


Figure 2. (A) TEM images of monodisperse Fe_3O_4 nanocrystals synthesized by the thermal decomposition in solvent with an increasing boiling point: (a) 5 nm, 1-hexadecene (b.p. 274 °C); (b) 9 nm, octyl ether (b.p. 287 °C); (c) 12 nm, 1-octadecene (b.p. 314 °C); (d) 16 nm, 1-eicosene (b.p. 330 °C) and (e) 22 nm, trioctylamine (b.p. 365 °C). Adapted with permission from [88], copyright 2004 Nature Materials. (B) SEM images of Fe_3O_4 NPs synthesized by solvothermal reaction. Adapted with permission from [90], copyright 2005 Angewandte Chemie. (C) TEM images of Fe_3O_4 NPs synthesized by hydrothermal reaction. Adapted with permission from [92], copyright 2013 Biomaterials. (D) TEM images of Fe_3O_4 NPs synthesized by microemulsion synthesis. Adapted with permission from [95], copyright 2006 Advanced Functional Materials. (E) TEM images of mesoporous Fe_3O_4 NPs synthesis by hard templates. Adapted with permission from [97], copyright 2008 Advanced Materials.

Table 2. Comparison of the different chemical synthesis methods of Fe_3O_4 NPs.

Method	Solvent	Reaction conditions	Process temperature	Process time	Shape control	Size distribution	Degree of crystallinity	Yield	Reference
Thermal decomposition	Organic solvent	N_2 atmosphere	High	Day	Very good	Narrow	High	High	[88, 89]
Solvothermal reaction	Organic solvent	High pressure	High	Hours	Bad	Narrow	High	High	[90]
Hydrothermal reaction	Water	High pressure	High	Hours	Bad	Relatively narrow	High	High	[92]
Coprecipitation synthesis	Water	N_2 atmosphere	Low	Minutes	Bad	Broad	Low	Medium	[93, 94]
Microemulsion synthesis	Oil/Water Water/Oil	N_2 atmosphere	Low	Hours	Good	Relatively narrow	Low	Low	[95]
Sol-gel synthesis	Organic solvent	N_2 atmosphere	Low	Hours	Good	Relatively narrow	Low	Medium	[96]
Template synthesis	Water	Normal pressures	High	Hours	Bad	Relatively narrow	Low	Medium	[97]

Solvothermal reaction/Polyol method

In order to prevent the self-aggregation and over-growth of monodisperse Fe_3O_4 nanocrystalline during the synthesis process, the decomposition of metal salts in organic solution-phase have been widely used [88, 89]. Based on this principle, the solvothermal method is extensively used to synthesize Fe_3O_4 NPs with low cost, simple operation, and excellent crystallinity. Li *et al.* [90] reported the method for the synthesis of hydrophilic, monodisperse, and single-crystalline magnetic ferrite (MFe_2O_4 ; M=Fe, Mn, Zn, or Co) microspheres by a

solvothermal reduction method, and the monodispersed ferrite spheres were controlled with the diameters from 200 to 800 nm (Figure 2B). This solvothermal method provides an important method to get monodisperse nanostructures without demanding a narrow size distribution. However, the final nanocrystals from oleic acid/amine during the solvothermal reaction usually coated with long alkyl chain oleic acids or amines with hydrophobic surface properties, which greatly inhibits their applications in biotechnological areas and others. In order to receive monodisperse and hydrophilic nanocrystals, ethylene glycol could be used as the solvent in the

solvothermal synthesis of magnetic ferrite nanocrystals with hexanediamine or polyethylene glycol as protecting reagents.

The polyol method is similarly developed to fabricated Fe₃O₄ NPs by using polyols (such as, diethylene glycol, ethylene glycol and triethylene glycol) to reduce the metal compounds to obtain the corresponding nanoparticles. In this method, the solvent of polyols with high boiling points can be used as both the reducing agents and the stabilizing agents to control the growth process of nanoparticles and prevent possible agglomeration [91]. Wan *et al.* [106] prepared monodisperse Fe₃O₄ NPs with a uniform size of 10 nm through the polyol method using the triglyceride glycol and iron acetylacetone, the obtained Fe₃O₄ NPs showed well dispersity in aqueous or other polar media due to hydrophilic polyol ligands coated in the synthesis process.

Hydrothermal reaction

Fe₃O₄ NPs can also be synthesized by the hydrothermal reaction under the condition of suitable temperature (100–250 °C) and relatively high pressure (0.3–4 MPa) [107]. Hydrothermal synthesis involves no organic solvents or metal organic precursors, and the high crystallinity and good hydrophilicity of yielded Fe₃O₄ NPs omits the subsequent surface modification processes [92]. Shi *et al.* [92] reports the facile preparation of Fe₃O₄ NPs coated with branched PEI (abbreviated as: Fe₃O₄-PEI NPs) *via* the hydrothermal method (Figure 2C). The surface of Fe₃O₄-PEI NPs with primary amine groups, which could be further modified with PEG, succinic anhydride and acetic anhydride, and induce Fe₃O₄-PEI NPs continue surface functionalities. Hydrothermal reaction provides a choice for the simple synthesis Fe₃O₄-based multifunctional nanomaterial for biomedical applications.

Coprecipitation synthesis/Sol-gel synthesis

Coprecipitation of Fe²⁺ and Fe³⁺ ions in solution also a classical method applied to manufacture Fe₃O₄ NPs by precipitating a specific proportion of the inorganic salts in aqueous media [79, 108]. Compared with the thermal decomposition synthesis, the coprecipitation can avoid the problem that surface decoration (template molecules, surface organic ligands, surfactant) are difficult to be removed [93, 94]. The size, quantity and morphology of the obtained Fe₃O₄ NPs could be controlled by experimental condition, such as power of hydrogen (pH), ion concentration, reaction temperature, precursor and so on. Stroeve *et al.* [109] synthesized the Fe₃O₄ NPs in aqueous solutions without any surfactants. The coprecipitation process of Fe²⁺/Fe³⁺

was achieved by changing the pH value of solution, and the achieved Fe₃O₄ NPs with a narrow size distribution and the average diameter less than 10 nm [98].

Sol-gel method can be considered as the further development from this strategy, which stirred the metal salt with a gelling agent to form a homogeneous gel, then gelled the sol by chemical reaction or solvent removal to get a 3D iron oxide network [96]. To obtain the pure Fe₃O₄ NPs, the formed gels usually requires an additional crushing step after drying and calcination. The structure and properties of the obtained Fe₃O₄ NPs are usually influenced by the concentration, reaction temperature, pH values, and solvents. The yield of nanoparticles using the sol-gel method usually is high, thus this method can be used for massively producing large-sized nanoparticles.

Microemulsion synthesis

Microemulsion method is also widely investigated as a classic method to prepare nanocrystals [110]. Microemulsion is a thermodynamically stable dispersions, which can be obtained by mixing immiscible water/oil phase that stabilized by the arrangement of co-surfactant or surfactant molecules at the interface. The microemulsion system especially the water-in-oil (W/O) phase, which is consist of the dispersion of water nanodroplets in the oil phase to form a stabilized spherical reverse micelle, can be considered as "nanoreactor" for the synthesis of nanoparticles. Since the nucleation and growth of nanoparticles are limited in the nanoreactor, that the size of nanoparticles can be controlled [111]. Li *et al.* [95] reported the synthesis of the magnetic Fe₃O₄ NPs by the W/O microemulsions, and investigated the relationship between the experiment condition (concentration, water/ethanol/organic solvent ratio, kinds of surfactants, temperature, reaction time) and the properties (morphology, crystal phase, and size distribution) of the obtained Fe₃O₄ NPs (Figure 2D).

Template synthesis

Recently, many researches have designed and prepared of hollow or porous Fe₃O₄ nanostructures by the template synthesis method, which can be divided into the hard template method (e.g., silica, carbon spheres, and polymer nanoparticles) and the soft template method (e.g., vesicles, micelles, emulsion droplets, gas bubbles and others) according with the process of package, calcination and separation in obtaining the hollow nanostructure [112]. Among the hard templates, polymer latex particles, especially polystyrene (PS) beads, have been demonstrated to be effective templates for the preparation the hollow

spherical inorganic materials of Fe₃O₄ NPs [113], and this method also be applied to other nanoparticles, such as Gd₂O₃ [105], TiO₂ [114], ZnS [115], SiO₂ [116] and so on. Similarly, mesoporous silica can also be used as the hard templates for the preparation of mesoporous Fe₃O₄ NPs, followed by the process of heating treatment and silica removal (Figure 2E) [97]. Compared to the hard template method, the morphology of Fe₃O₄ NPs synthesized by the soft template method is usually more uncontrollable. The obtained Fe₃O₄ NPs usually present nanowires structure and are rarely used in cancer diagnosis and treatment.

Surface Modification of Magnetic Fe₃O₄ NPs

Fe₃O₄ NPs prepared with hydrophobic ligands (oleic acid or stearic acid) needed to be converted into hydrophilic ligands for further biomedical applications [104]. Meanwhile, appropriate surface modification can also import the Fe₃O₄ NPs with better biocompatibility, long blood circulation and further functionalization, such as active targeting ability [105, 117]. Currently, the surface modification methods of Fe₃O₄ NPs fall into two categories of ligand replacement and encapsulation [118, 119]. Ligand replacement refers to an exchange of native hydrophobic ligands (oleic acid) on the surface of nanoparticles with strong anchoring groups (such as

phosphonates, catechols, thiols, sulfonates, and carboxylic acids), which act as hydrophilic ligands to improve their dispersity in biological environment [120-123]. However, the actual ligand exchange process is often underperformed and always causes the leakage of surface ligand defectiveness. In contrast, the surface modification of Fe₃O₄ NPs through the encapsulation method shows better efficient, which can effectively coating the surface of Fe₃O₄ and ensure their uniformity [124, 125]. The usual strategy of encapsulation process is to utilize inorganic or organic shells to embellish iron oxide nanoparticles into core-shell structured nanocarriers [126-128], and the surface functionalized decorations mainly include noble metals (e.g., gold, silver, gadolinium) [129-132] or oxides (e.g., silica, graphene, titanium dioxide) [133, 134], biodegradable organic polymers (e.g., polyethylene glycol (PEG), poly (lactic-coglycolicacid) (PLGA)) [135-137], proteins (e.g., antibodies, monoclonal antibody and their fragments) [138], nucleic acids (e.g., DNA, siRNA, aptamers) [134, 139-141], amino acids (e.g., phenylalanine, tyrosine, arginine, lysine and cysteine) [142], small molecules (e.g., photosensitizer, folic acid, doxorubicin), and other species (vitamins, carbohydrates) [143, 144]. Here we detailly introduce the recent advances in the surface modification Fe₃O₄ NPs (Table 3).

Table 3. Comparison of different modification methods of Fe₃O₄ NPs.

Variety	Name	Modification methods	Cost	Shape control	Size distribution	Treatment of type	Reference
Mesoporous material	SiO ₂ , Si	Sol-gel	Low	Easy	Narrow	Drug delivery	[148-152]
Photosensitizer	TiO ₂ , Ce6	Hydrothermal method, Adsorption	Low	Moderation	Broad	PDT	[228-229]
Noble metal	Ag, Pt, Bi	Hydrothermal method	High	Easy	Narrow	PTT	[155-160]
Polymer	PEG, PLGA	Ligand exchange	Moderation	Moderation	Narrow	PDT Drug delivery	[165-169]
Metal-organic frameworks	ZIF-8, MIL-100(Fe)	Hydrothermal method In-situ synthesis	Low	Moderation	Broad	Drug delivery PDT	[171-173]
Liposome	cytmembrane, , phosphatide	Extrusion method, Biosynthetic	Moderation	Hard	Broad	Drug delivery	[181-184]
Biomacromolecule	siRNA, Aptamer	Adsorption, assemble	High	Hard	Broad	immunotherapy	[186][251-256]
Micromolecule	FA, DOX	Adsorption, assemble	High	Easy	Narrow	Drug delivery	[242-250]

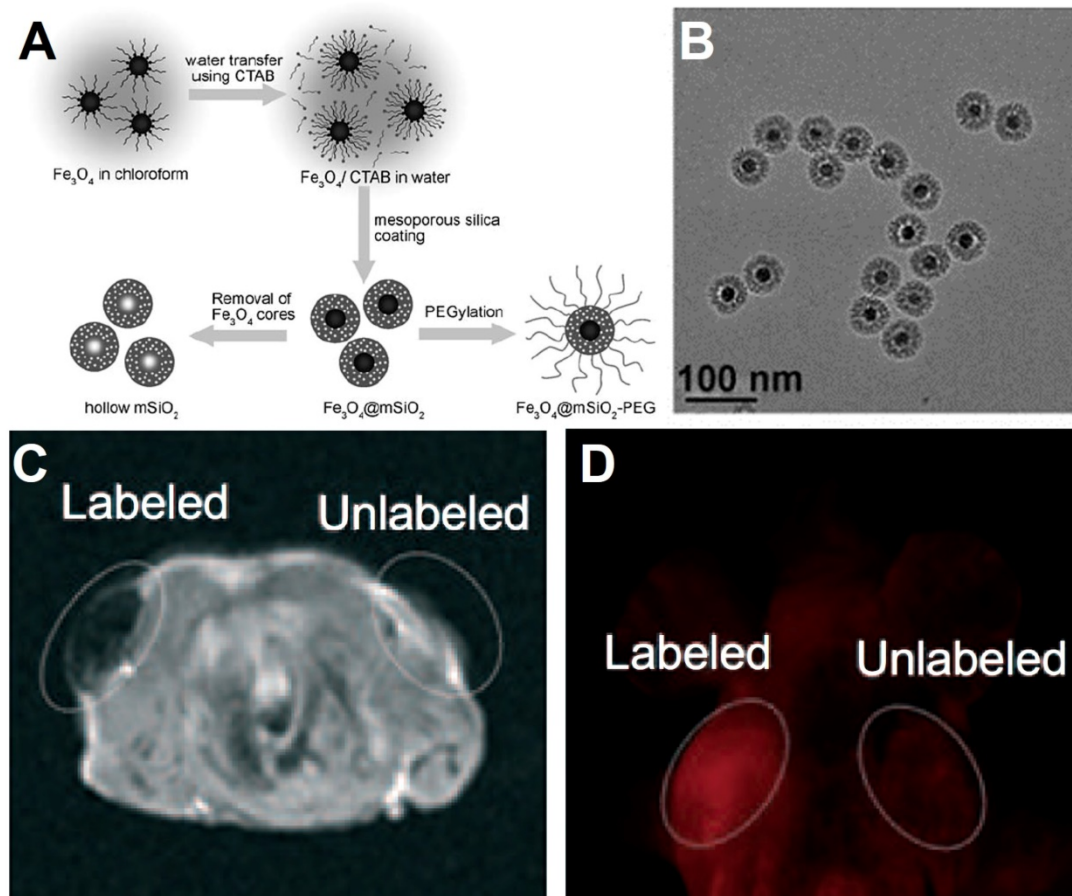


Figure 3. (A) Synthetic schematic illustration of core-shell structure Fe₃O₄@mSiO₂ NPs. (B) TEM image of Fe₃O₄@mSiO₂ NPs. *In vivo* imaging for the T₂-weighted MRI imaging (C) and fluorescence confocal microscopy image (D) using Fe₃O₄@mSiO₂. Adapted with permission from [153], copyright 2008 Angewandte Chemie International Edition.

Inorganic mesoporous materials

In recent years, many inorganic nanomaterials have been extensively studied in biomedical fields, such as silica, aluminum oxide, molybdenum dioxide, graphene, calcium carbonate, calcium phosphate and others [145-147]. Among them, mesoporous silica (mSiO₂) materials have been used as delivery carriers for small molecule drugs, quantum dots, siRNA and aptamers due to their uniform pore sizes and high accessible pore volume [148, 149]. Meanwhile, the monodisperse mSiO₂ smaller than 100 nm, have also been proved to possess a high stability in blood circulation [150-152]. The modification of mSiO₂ onto Fe₃O₄ NPs to form uniform core-shell nanocomposite have been reported to improve their biocompatible, enhance hydrophilicity and provide anchoring points (Si-OH groups) for further loading of molecular drugs (e.g. paclitaxel, platinum-based drugs, DOX) or other targeted functional groups (e.g. FA, antibodies). The modification of mSiO₂ shell onto Fe₃O₄ NPs usually using the sol-gel method or microemulsion method. Hyeon *et al.* [153] synthesized the composite structure consist of monodisperse Fe₃O₄ NPs core and mSiO₂ shell (Figure 3). CTAB was used as the surfactant for

the transfer of hydrophobic Fe₃O₄ NPs, and provide the soft template for the grown of mSiO₂ shell in the sol-gel process. The size of Fe₃O₄@mSiO₂ NPs could be controlled within 100 nm, and the fluorescein isothiocyanate and rhodamine B isothiocyanate were further modified on the mSiO₂ shell for fluorescence imaging *in vivo*, which could show typical emissions of fluorescein and rhodamine B at 516 nm and 577 nm with the corresponding excitation wavelength of 460 nm and 520 nm. Meanwhile, the core-shell Fe₃O₄@mSiO₂ NPs also could be used as the contrast agent for T₂-weighted MRI *in vivo*, providing an idea for construction multimodal imaging platform by modifying the hydrophobic Fe₃O₄ NPs with the functional mesoporous material shell.

Noble metals

Magnetic Fe₃O₄ NPs, due to their excellent imaging properties and magnetic targeting ability, are usually conjunction with other functional systems to improve their capability for multimodal imaging and precision targeting [154]. Among them, noble metals are a crucial species of functional components. On one hand, most of noble metals have a higher atomic number than the iodine element, and can be used as

the contrast agent for computed tomography (CT) imaging, due to their remarkable X-ray attenuation property [155, 156]. On the other hand, noble metals usually have the strong surface plasmon resonance (SPR) effect, which could absorb the energy of light and convert that into thermal or other energy [157]. In particular, the core/shell nanostructures adopt the plasmonic effects of noble metals into magnetic Fe_3O_4 NPs, can be used in the photothermal therapy of cancer [158-160]. Shi *et al.* [157] developed a multifunctional theranostic nanoplatforms for tumor imaging and therapy based on the star-shaped Fe_3O_4 @Au core/shell nanoparticles, which presented an excellent effect in MRI, CT, thermal imaging and photothermal therapy. After further modification of PEI and HA, the nanostars showed better biocompatibility, stability and targeting for cancer cells.

Shi *et al.* [158] reported a method for preparation the core-shell structured of Fe_3O_4 /Au, and the Fe_3O_4 NPs core are linked to the Au shell by the hybrid of SiO_2 and PS-b-PAA (a kind of amphiphilic block copolymers consisting of polystyrene and polyacrylic acid). The details of synthetic process are shown in Figure 4A. First process is modified SiO_2 on the surface of Fe_3O_4 NPs and self-assembly with the PS-b-PAA. Then reduce AuCl_4^- on the surface of

Fe_3O_4 @hybrid to Au NPs form the shell structure, and ultimate formation the Fe_3O_4 /Au. The SPR effect of Au NPs on the core-shell structured could absorb the near-infrared light (808 nm) and converted that into thermal energy and eventually kill the tumor cells. Meanwhile, due to the MRI performance of the Fe_3O_4 , the noble metal modified Fe_3O_4 not only have property of photothermal therapy, but also an agent of MRI and thermal imagery, demonstrating a flexible way for the construction of Fe_3O_4 -based multifunctional diagnosis and treatment platforms.

Polymers

In the last decade, biocompatible polymers have been extensively used to improve conventional mode of medication in drug-delivery [161-163]. Meanwhile, the magnetic Fe_3O_4 NPs are gaining more research interests in the medical fields relying on their unique properties such as imaging capability of MRI and magnetic targeting drug carrier. For improving the hydrophilicity and other physiochemical properties of Fe_3O_4 NPs, the surface modification with polymers provided an ideal choice, and the commonly used polymers include polyethylene glycol (PEG), poly(L-lysine) (PLL) [164], poly(propyleneimine) (PPI), polyethylenimine (PEI), polystyrene (PS) [165], poly(vinyl pyrrolidone) (PVP), poly(lactic-co-glycolic

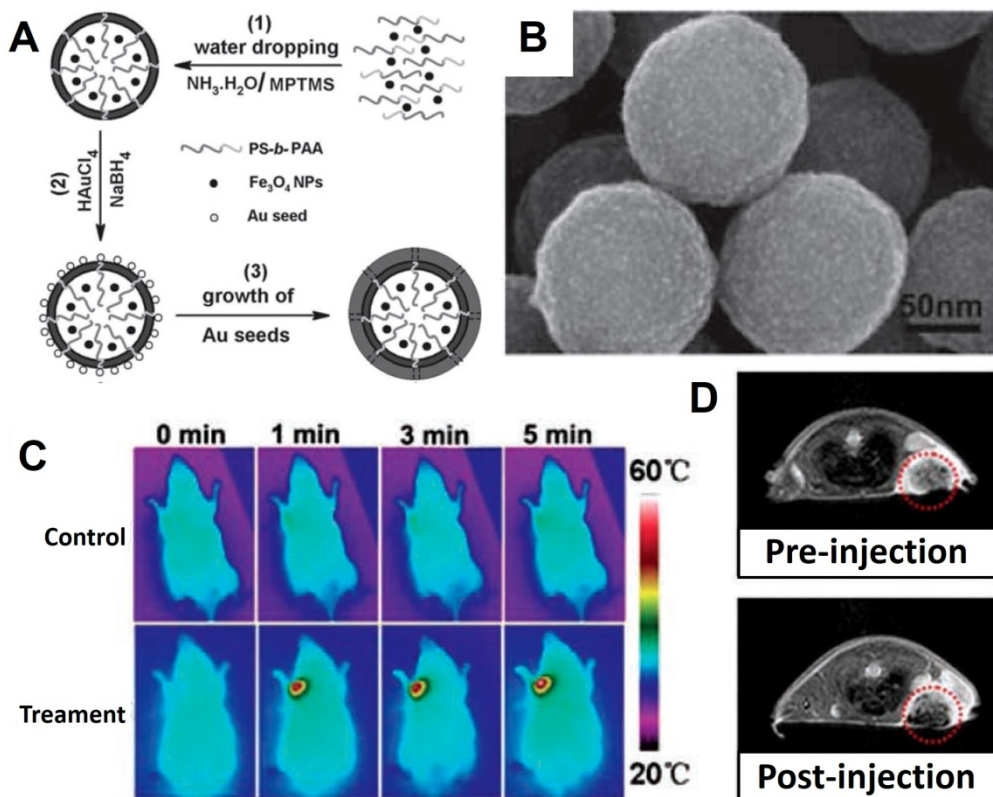


Figure 4. (A) Schematic of synthesis Fe_3O_4 /Au nanocomposite. (B) SEM images of Fe_3O_4 /Au core-shell structure. (C) Thermal images effect of Fe_3O_4 /Au nanocomposite under 808 nm irradiation. (D) The T_2 -weighted MRI effect of Fe_3O_4 /Au nanocomposite *in vivo*. Adapted with permission from [158], copyright 2011 Advanced Materials.

acid) (PLGA) and poly (vinyl alcohol) (PVA)), which having hydrophilic segments to improve biodegradability and biocompatibility. Parveen *et al.* [166] revealed the surface coated Fe_3O_4 NPs with the hydrophilic PEG could prevent nanoparticles from being removed by the phagocytic activities to further boost the endurance of the Fe_3O_4 . PLGA is a biodegradable polymer and has been frequently used as a drug-delivery platform in the treatment of cancer therapy in recent years, and has also been reported to modify magnetic Fe_3O_4 NPs for enhance their magnetic targeting delivery ability to tumor tissues under magnetic field conditions [167-169]. Wu *et al.* [170] prepared the uniform microcapsules with Fe_3O_4 and PEGylated PLGA (abbreviated as $\text{Fe}_3\text{O}_4@\text{PEG-PLGA MCs}$) for MRI and ultrasound bimodal imaging (USI) (Figure 5). The $\text{Fe}_3\text{O}_4@\text{PEG-PLGA MCs}$ showed better stability in physiological solutions owing to the PEGylation. Meanwhile, the *in vivo* and *in vitro* experiment results showed the polymers modified Fe_3O_4 -based microcapsules could be used as an agent for USI and MRI performance, without dramatic cytotoxicity and embolism to mice even at high doses.

Metal-organic frameworks

Metal-organic frameworks (MOFs) is an emerging species of porous nanomaterials acquire from metal ions or clusters coordinating with bridged ligands, which could be used to load guest nanoparticles to gain new performance due to their good physicochemical stability, larger surface area and tunable functionality [171]. Responsive MOFs coated Fe_3O_4 NPs have been studied for improving the hydrophilicity, increasing the porosity of delivery system and enhancing the responsiveness of the tumor environment. The mechanism of MOFs responsive decomposition may be due to the effects of H^+ and glutathione (GSH) in the tumor microenvironment on the binding of metal ions and organic ligands [171, 172]. Yang *et al.* [172] designed a novel MRI contrast agent, which utilized the pH and GSH responsive ZIF-8 as nanocarrier to deliver small-sized Fe_3O_4 NPs (about 5 nm, T_1 -weight MRI) into a Fe_3O_4 -ZIF-8 nanostructure (T_2 -weight MRI). The slightly acidic conditions and overexpressed GSH in tumor microenvironment would lead the decomposition of the Fe_3O_4 -ZIF-8 nanostructure and release the small-sized Fe_3O_4 (Figure 6A), leading to

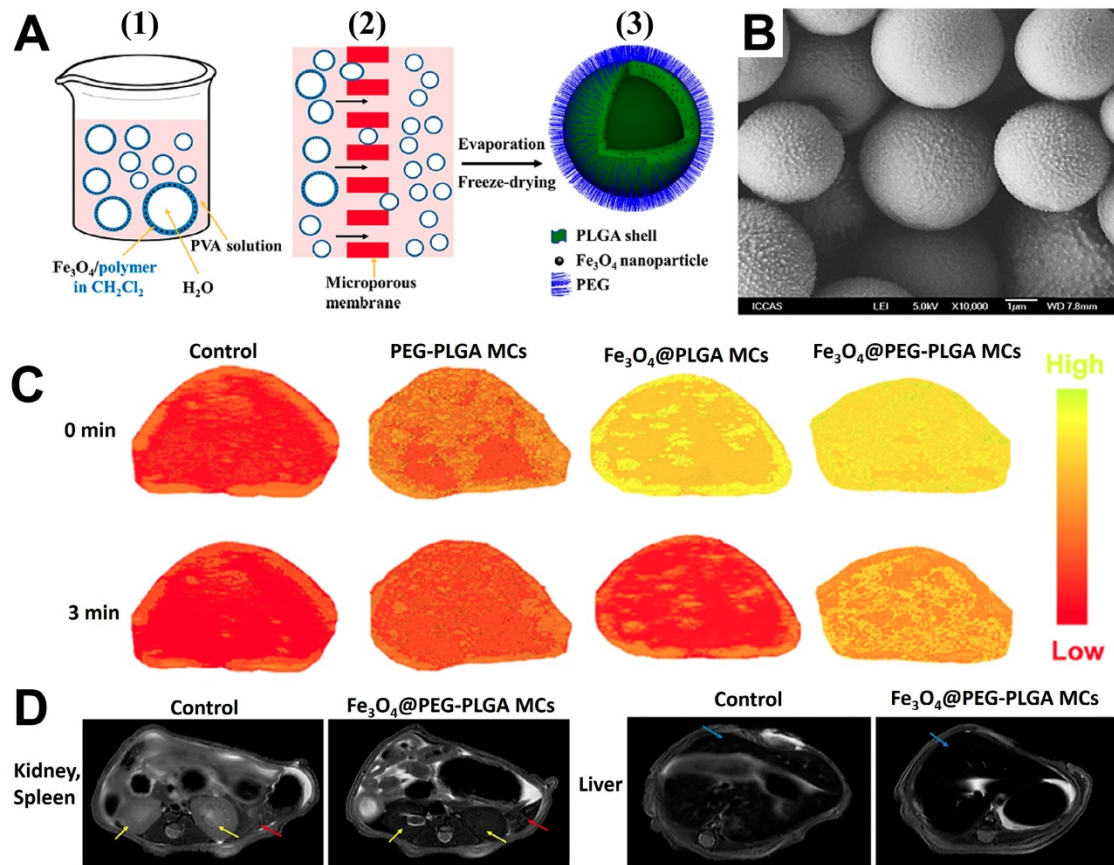


Figure 5. (A) The schematic diagram: (1) The traditional method yielded microcapsules with an uneven distribution; (2) Premix membrane emulsification method obtained uniform microcapsules with the help of microporous membrane; (3) The structure diagram of $\text{Fe}_3\text{O}_4@\text{PEG-PLGA MC}$. (B) SEM images of $\text{Fe}_3\text{O}_4@\text{PEG-PLGA MCs}$. The imaging of *in vivo* USI (C) (liver) and MRI (D) of mice. Arrows of yellow, red and blue corresponding to kidneys, spleens and livers. Adapted with permission from [170], copyright 2015 ACS Applied Materials & Interfaces.

the MRI effect from T_2 to T_1 and enhancing the contrast of the tumor tissue (detail in part 4.3), which could distinguish tumor tissue from the normal tissue by the T_2 to T_1 conversion. Han *et al.* [173] synthesized a novel Co-ferrocene metal-organic framework (Co-Fc MOF) with high Fenton activity. After combined with the glucose oxidase (GOx), the nanoplatform (Co-Fc@GOx) construct an enzymatic/Fenton catalytic synergistic effect for enhanced tumor treatment effect. GOx delivered by Co-Fc MOF could catalyze endogenous glucose of tumor microenvironment to H_2O_2 and gluconic acid, which further favored the Fenton reaction of Co-Fc MOF and enhanced the generation of ROS. Experimental results demonstrated this synergistic enzymatic/Fenton catalytic activity triggered by Co-Fc@GOx nanoplatform enabled remarkable anticancer properties both *in vivo* and *in vitro*.

Cell membranes and derivatives

It is a common method to functionalize the nanoparticles with tumor imaging and therapy with the exogenous ligand. However, several problems are still needed to be solved, such as: (1) the foreign nanoparticles can be easily detect by immune systems and cause severe immune responses; (2) the physiological barriers could eliminate nanomaterials from the blood circulation and restrict the accumulation in target sites; (3) nontargeted nanomaterials that relies on the EPR effect limit the therapeutic effects and increase the damage to normal

tissues; (4) the potential toxicity of nanomaterials *in vivo* [174-180]. Fe_3O_4 NPs with their unique properties and long blood circulation time are widely researched to overcome these limitations. Compared to exogenous ligands for surface modification, the endogenous cell membranes for nanoparticles wrapping provide a novel method for solve these problems [181-184]. The classic types of biomimetic cell membranes include red blood cell membrane, white blood cell membrane, cancer cell membrane, stem cell membrane and so on [185]. Zhao *et al.* [183] fabricated the delivery platform based on the platelet mimicking Fe_3O_4 NPs for enhancing the blood circulation time and targeting ability. As shown in Figure 7, step 1 showed the collections of blood from the mice, step 2 showed the dissociation of membrane and protein from platelet formed the vesicles, step 3 was to coat the vesicles of platelet on the surface of Fe_3O_4 NPs, step 4 was to injection the vesicles modified Fe_3O_4 NPs into blood vessel, steps 5 to 7 were the systematic circulation of vesicles modified Fe_3O_4 NPs, enrichment in tumor tissues by EPR effect and entry into tumor cells with the help of vesicles, steps 8 and 9 showed the performance test of imaging and therapeutic by the MRI and photothermal therapy (PTT). The results showed that the cell membrane modified Fe_3O_4 NPs have a good tumor targeting ability and could kill the tumor cells by photothermal treatment under the irradiation of near infrared light.

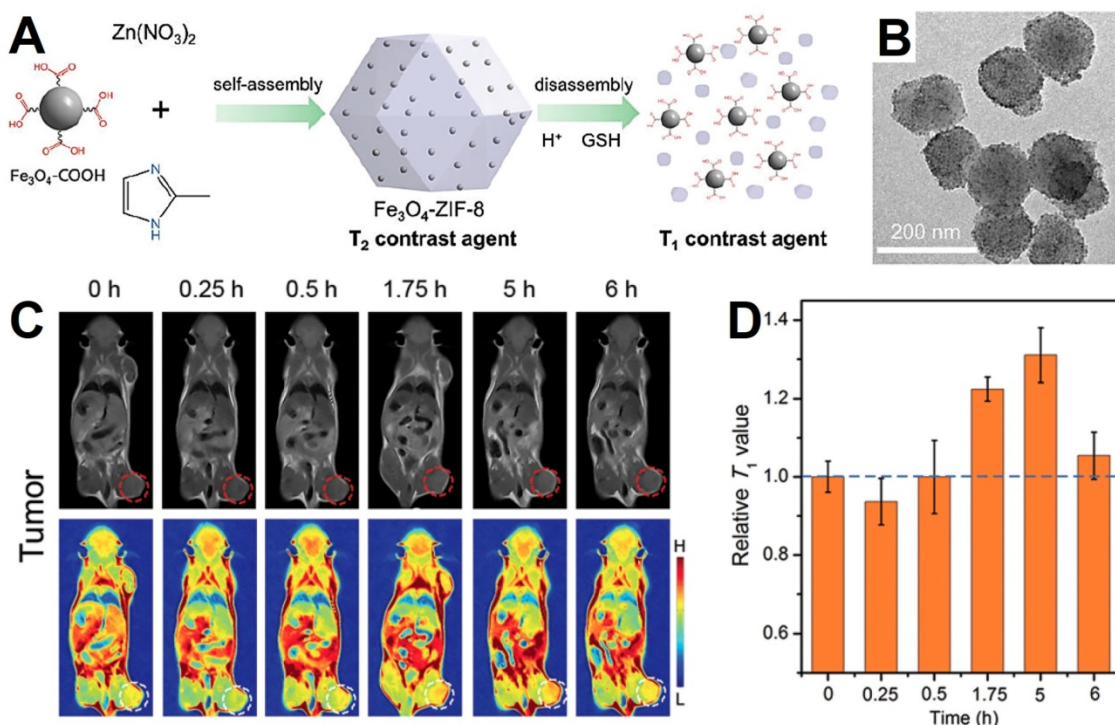


Figure 6. (A) Schematic of Fe_3O_4 -ZIF-8 switch from T_2 to T_1 weight. (B) TEM images of Fe_3O_4 -ZIF-8 assemblies. (C) *In vivo* T_1 -weight MRI of tumor after intravenous injection of Fe_3O_4 -ZIF-8, and homologous T_1 signals (D) extracted from tumor sites. Adapted with permission from [172], copyright 2019 Chemical Communications.

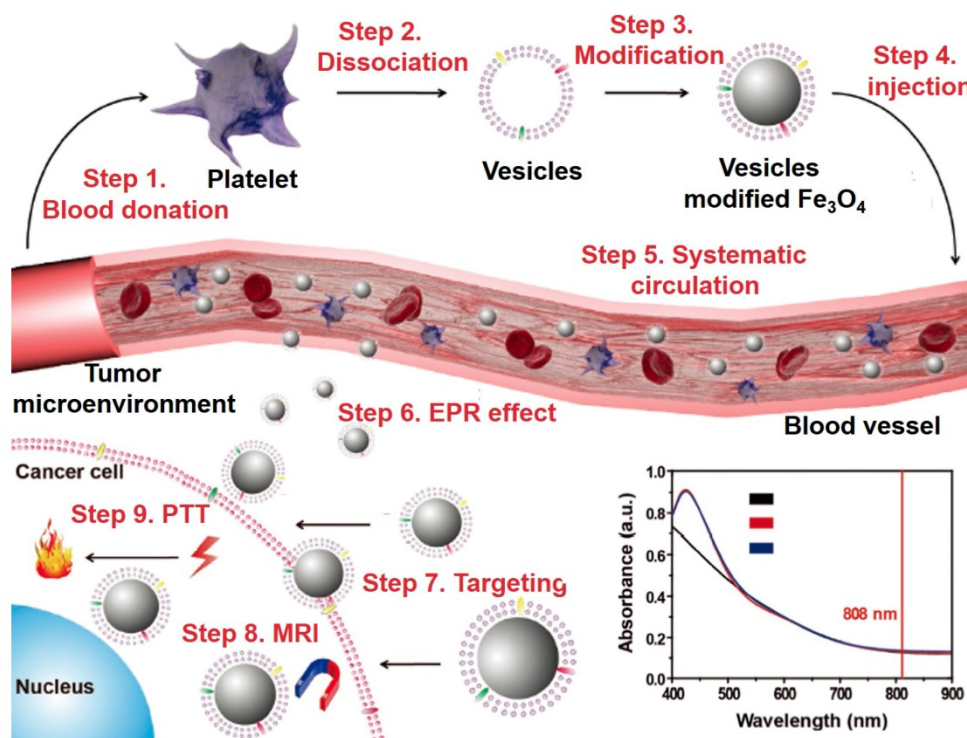


Figure 7. The schematic of platelet vesicles modified Fe_3O_4 NPs for enhanced the effect of MRI and PTT, and the UV-Vis-NIR absorption spectra of Fe_3O_4 NPs. Adapted with permission from [183], copyright 2017 Advanced Functional Materials.

Aptamers

In general, when the Fe_3O_4 NPs circulate in the blood system, they are easily subjected to macrophage uptake and reticuloendothelial system clearance. To improve specificity and recognition of the tumor targeted delivery system, many functionalized substances such as aptamers, peptides and small molecule can also be used for the surface modification of nanoparticles. Aptamer is a single-stranded oligonucleotide generated from an *in vitro* selection process, which called systematic evolution of ligands by exponential enrichment (SELEX) and they could bind with the targeted small molecules, proteins, and even intact cells and tissues with excellent specificity and high affinity. Aptamers used for surface modification have many advantages, such as easy to operate, good stability, rapid tissue penetration and lack of immunogenicity, thus making them as a suitable candidate. Tan *et al.* [186] designed a multifunction delivery platform that perform five distinct functions synergistically and effectively. To accomplish this, they prepared the gold-coated rose-shaped Fe_3O_4 ($\text{Au}@\text{Fe}_3\text{O}_4$) nanoplatform as an agent for photothermal therapy (PTT) and MRI. To enhance the targeting ability, the sgc8 aptamers were easily conjugated with the $\text{Au}@\text{Fe}_3\text{O}_4$ via the thiolate bonding, which could specifically recognize CCRF-CEM leukemia cells. Additionally, the chemotherapeutic agent doxorubicin (DOX) could

also intercalate into the GC base pairs in the extended part of the aptamers, and with the releasing of DOX, the fluorescence signal *in vitro* also changed and cause the optical imaging. Therefore, the DOX-loaded $\text{Au}@\text{Fe}_3\text{O}_4$ nanoplatform presented five distinct functions for simultaneous imaging and therapy with the help of aptamers.

Fe_3O_4 NPs for Tumor Imaging

T_2 -weighted magnetic resonance imaging

MRI is an effective method for tumor diagnosis due to the acquired high contrast images and the precise handling of details of the targeted tissues with non-invasiveness and real-time monitoring [184]. The sensitivity of MRI could be significantly enhanced with the help of contrast agents. The agents of MRI could be classified base on the effect on longitudinal (T_1) or transversal (T_2) relaxations, and the ability is defined as relaxivity (r_1, r_2). Therefore, MRI contrast agents could be divided in two types, which are T_1 -weighted (positive) and T_2 -weighted (negative), mainly shortens the T_1 and T_2 contrast media. In general, fast T_1 -weighted results appear to be bright contrast in the MRI, while the opposite T_2 -weighted results to be the dark contrast [187]. Due to the superparamagnetic property, Fe_3O_4 NPs typically decrease the relaxation time of surrounding protons, thus providing possibility to be employed as T_2 -weighted MRI agent media.

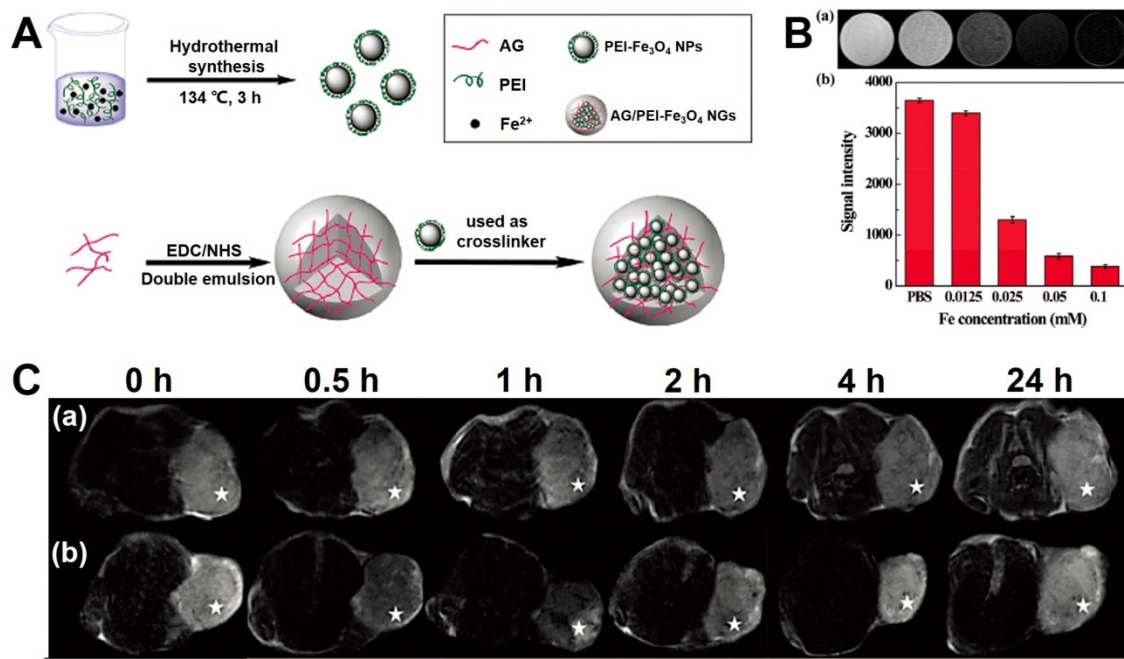


Figure 8. (A) The schematic of the synthetic process of AG/PEI-Fe₃O₄ NGs. (B) The imaging of *T*₂-weighted MRI *in vitro* (a) and signal intensity analysis (b). (C) The images of *T*₂-weighted MRI *in vivo*. Adapted with permission from [188], copyright 2016 Biomaterials Science.

Shi *et al.* [188] prepared a novel agent for MRI, which was the nanogels consisting of PEI coated Fe₃O₄ NPs immobilized with alginate (abbreviated as: AG/PEI-Fe₃O₄ NGs). The synthetic process is shown in Figure 8, and the nanogels presented a dispersion state in water with the size distribution from 153 nm to 219.2 nm. Moreover, the novel Fe₃O₄-based nanogels were excellent *T*₂-weighted contrast agent for the MRI (the relaxivity of *r*₂ is 170.87 mM⁻¹s⁻¹) and could be vastly swallowed by the tumor cells.

***T*₁-weighted magnetic resonance imaging**

Superparamagnetic Fe₃O₄ NPs (SPIONs) are widely used as *T*₂ contrast agents, since the strong magnetic moment could lead the magnetic inhomogeneity. However, some reasons limit their clinical application of *T*₂ contrast agents [189]. Because the intrinsic dark signal of *T*₂-weighted MRI could not accurately distinguish the tumors and other hypointense areas, such as calcification, metal deposition, or bleeding. Meanwhile, the *T*₂-weighted contrast agents usually with the high magnetic moment that perturbation the local magnetic field, which could exaggerate the size of the labeled area and blurs the images, thus causing the so-called “blooming effect”. Therefore, *T*₁ contrast agents shows better desirable than *T*₂ contrast agents for the accurate and high-resolution imaging [190]. It is noteworthy that compared with the familiar *T*₁ contrast agents, Fe₃O₄ contrast agents show better biocompatibility due to the iron element are rich in human blood, and stored in the body in the form of

ferritin [201]. However, the common Fe₃O₄ NPs are unfit for the *T*₁ contrast agents because of that the ideal *T*₁ contrast agents would have high *r*₁ value and low *r*₂/*r*₁ ratio to realize the *T*₁ contrast maximize effect [191]. Although iron with five unpaired electrons which could increase the *r*₁ value, the innate high magnetic moment of Fe₃O₄ NPs lead to the high *r*₂ value and prevents then to be used as *T*₁ contrast agent. However, this problem could be solved by decreasing the size of the Fe₃O₄ NPs, because the magnetic moment of Fe₃O₄ NPs could rapid decreases with the sizes reduction, which can lead to the reduction in the volume magnetic anisotropy [41, 192-194]. Therefore, a series of research on Fe₃O₄ NPs as contrast agent are widely carried out.

Hyeon *et al.* [189] reported the preparation of small-sized Fe₃O₄ NPs (mainly 3 nm) by the thermal decomposition (Figure 9), and the obtained Fe₃O₄ NPs showed extremely low magnetization derived due to the spin canting effect. For improving the water-dispersion and biocompatibility of Fe₃O₄ NPs, the PO-PEG ligands were modified on the surface. *In vitro* cytotoxicity assay of PO-PEG capped Fe₃O₄ NPs showed no observed toxic response, exhibited a high *r*₁ relaxivity (4.78 mM⁻¹ s⁻¹) and low *r*₂/*r*₁ ratio (6.12), which demonstrated the magnetic Fe₃O₄ NPs could be used as *T*₁ contrast agents. The high *r*₁ relaxivity of Fe₃O₄ NPs could be attributed to the large surface number of iron with five unpaired valence electrons. The Fe₃O₄ NPs (around 3 nm) indicated a longer circulation time than the clinically used Gd-based contrast agents. High-resolution blood pool MRI

using Fe_3O_4 NPs were able to provide a clear observation of various blood vessels within sizes less to 0.2 mm. All of these results demonstrated the Fe_3O_4 NPs with the potential as T_1 contrast agents for MRI in clinic.

However, there are still several problems limit the ultrasmall size Fe_3O_4 NPs used as T_1 contrast agents [195]. First, ultrasmall size nanoparticles could be fast cleared out by renal metabolism and limit the imaging. Second, due to the high surface energy, the self-aggregation is a major concern of ultrasmall nanoparticles. Once aggregated the small Fe_3O_4 NPs will lose their T_1 performance. Third, the surface modification of the ultrasmall size Fe_3O_4 NPs is

critical to maintain the T_1 performance, because the molecules modified on the surface directly controls the paramagnetic [195, 196]. Therefore, it is necessary to modify the ultrasmall size Fe_3O_4 NPs reasonably while ensuring its performance. Bao *et al.* [196] reported a novel method to form nanoclusters by crosslinking bovine serum albumin (BSA) onto ultrasmall size Fe_3O_4 NPs (Figure 10). Different from traditional studies showing T_1 signal decrease or complete loss after polymer encapsulation, the nanoclusters not only maintain the T_1 contrast agent's performance of the Fe_3O_4 NPs, but also significantly enhanced the blood circulation times from 15 minutes to over two hours.

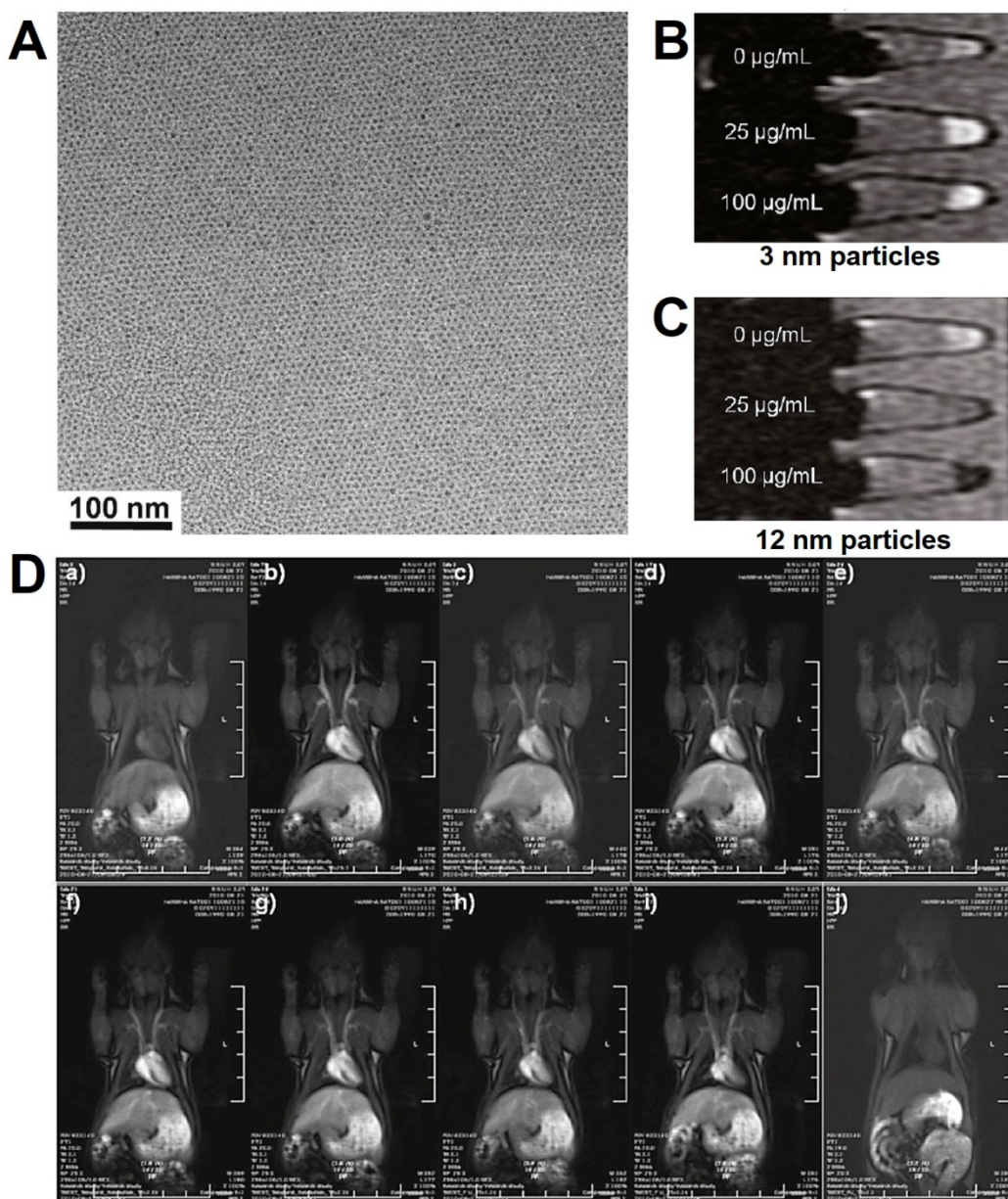


Figure 9. (A) TEM images of Fe_3O_4 NPs; T_1 -weighted MRI of Fe_3O_4 NPs with the diameters of 3 nm (B) and 12 nm (C); (D) The MRI intensity with the dynamic time *in vivo*. Adapted with permission from [189], copyright 2011 Journal of the American Chemical Society.

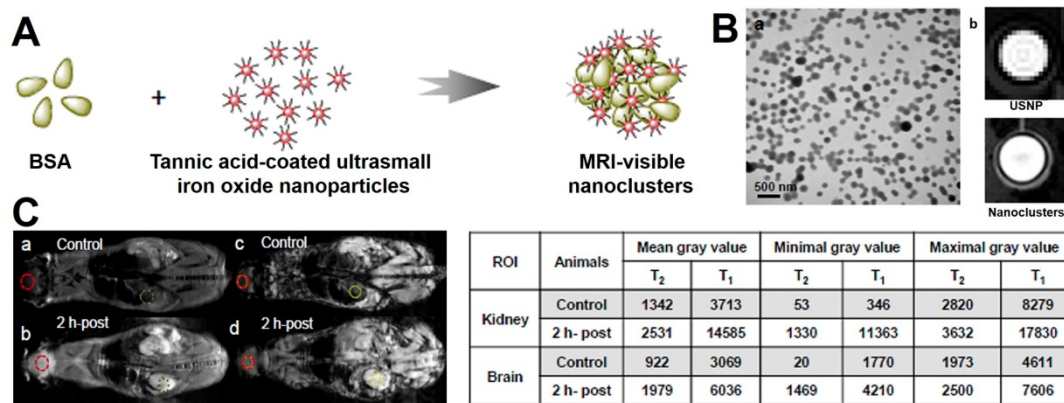


Figure 10. (A) The synthetic process of BSA modified Fe_3O_4 nanoclusters. (B) (a) TEM image of BSA modified Fe_3O_4 nanoclusters, (b) T_1 -weighted MRI of ultrasmall size Fe_3O_4 NPs (USNP) and BSA modified nanoclusters. (C) T_2 and T_1 -weighted MRI after injection for 2 hours, the measured gray values of kidney and brain regions are shown in table. Adapted with permission from [196], copyright 2017 Nanoscale.

4.3 Responsive T_1/T_2 imaging

Due to the fact that magnetic Fe_3O_4 NPs display a remarkable change from the T_2 enhanced contrast effect to T_1 enhanced contrast effect when the size less than 5 nm, Fe_3O_4 NPs have become an attractive material for the preparation of responsive MRI contrast agents for tumor diagnosis. Yang *et al.* [172] utilized the ZIF-8 as a carrier for agglomerate small Fe_3O_4 NPs (a T_1 contrast agent) into Fe_3O_4 -ZIF-8 assembly (a T_2 contrast agent). Because ZIF-8 is more stable under the normal physiological conditions and decompose under the acidic microenvironment of tumor tissues or in the presence of competitive ligands (Figure 6A). Therefore, the acidic conditions and GSH of the tumor microenvironment would trigger the disassembly of Fe_3O_4 -ZIF-8 and to release the ultrafine size Fe_3O_4 NPs, leading the conversion from T_2 to T_1 enhancement on the sign of the tumor tissue.

The low delivery efficiency of nanomaterials is still a challenge in tumor imaging and treatment. Generally speaking, the EPR effect is considered as a driving force through either active or passive targeting for nanoparticles to reach and accumulate in the tumor tissues. Previous research has shown that nanoparticles in appropriate sizes (from 50 nm to 200 nm) can enhance the EPR effect through limit nanoparticle extravasate back into the circulation. Recently, more and more researches have been proved the mutual effect between nano system and the biological environment also affect the effect of nanomaterials and the mount of accumulation in tumor, some modified ultrafine size nanoparticles show better permeation and distribution in the tumor tissue than large nanoparticles, which include the size less than 5 nm Fe_3O_4 T_1 -contrast agent. Mao *et al.* [197] reported a research using the Fe_3O_4 NPs (3.5 nm) modified with oligosaccharide (uIONPs), which could

penetrate the tumor tissue and self-assemble in the acidic microenvironment of tumor tissues (Figure 11). The improvement on the delivery and tumor retention of Fe_3O_4 NPs were achieved by combining the reduced intravasation and enhanced extravasation. Moreover, *in vivo* MRI revealed that ultrafine Fe_3O_4 NPs showed “bright” T_1 contrast when injected into the tumor vasculature, and then turn into “dark” T_2 contrast after 24 h. The switch of T_1-T_2 contrast demonstrated the ultrafine Fe_3O_4 NPs with T_1 contrast were dispersed state when inject into blood, and may aggregate formed large size Fe_3O_4 clusters with T_2 contrast after penetrated into the tumor tissues. Therefore, this property of Fe_3O_4 NPs showed an inspiration on the design of responsive T_1/T_2 conversion MRI contrast agents.

4.4 Multimodal imaging

In the process of the diagnosis and treatment, single imaging modality often cannot provide complete information about the tissues and organs [194]. Therefore, the combination of Fe_3O_4 NPs with two or more components to construct multimodal imaging system has become one of the main research directions [108]. Liu *et al.* [198] have designed the core-shell structure of $\text{Fe}_3\text{O}_4@\text{Cu}_{2-x}\text{S}$ (<10 nm), which showed excellent superparamagnetic and photothermal conversion capability. Therefore, the $\text{Fe}_3\text{O}_4@\text{Cu}_{2-x}\text{S}$ nanoparticles could be used as the agent of MRI, thermal imaging and photothermal therapy. Lee *et al.* [199] designed a MRI agent by the construction of $\text{Fe}_3\text{O}_4/\text{MnO}$ nanoparticles to implement the dual modes of T_2 and T_1 contrast enhancement of each compound. The *in vitro* and *in vivo* results that the dumbbell-shaped $\text{Fe}_3\text{O}_4/\text{MnO}$ nanoparticles with negative T_2 contrast effect in the full state, but in low pH environment, the positive effect of T_1 -weighted MRI was raised due to the releasing of Mn^{2+} . Yang *et al.* [200] have designed a

multifunctional nanoplatform by assembly the upconversion nanoparticles (UCNPs: $\beta\text{-NaGdF}_4\text{:Yb}/Tm@\beta\text{-NaGdF}_4$) on the surface of graphitic-phase carbon nitride ($g\text{-C}_3\text{N}_4$) coated Fe_3O_4 nanospheres (Figure 12). Due to the T_1 contrast agents of Gd and T_2

contrast agents of Fe, this platform showed the magnetic targeting ability under the guide of external magnetic field, and further supervised the therapeutic effect by dual-modal imaging precise localization.

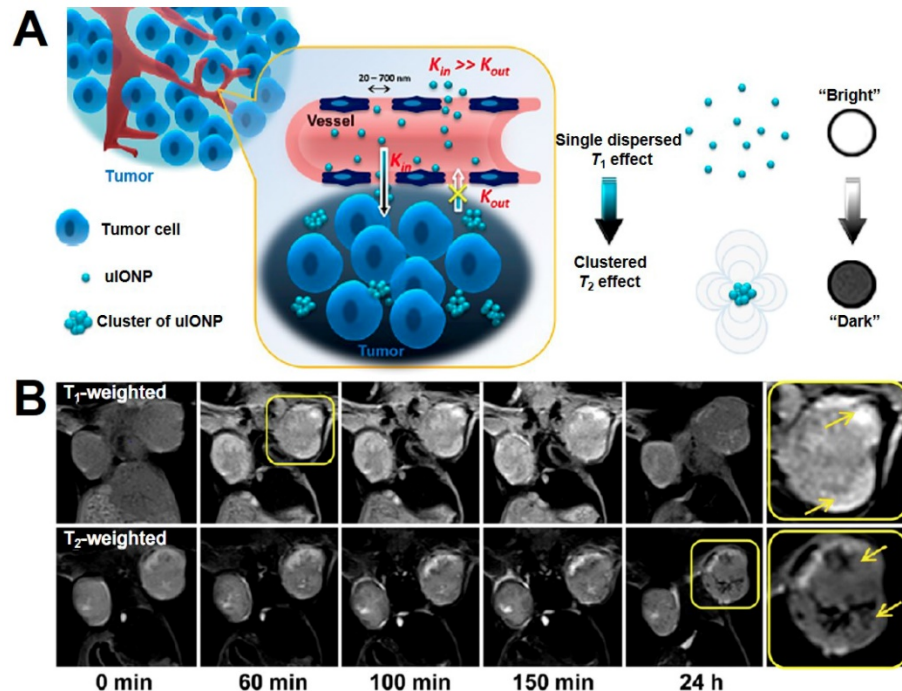


Figure 11. (A) The mechanism diagram of ultrafine Fe_3O_4 NPs (uIONPs) switch from T_1 - T_2 . (B) The change of T_1 to T_2 -weighted MRI *in vivo* after injecting uIONPs for different times. Adapted with permission from [197], copyright 2017 ACS Nano.

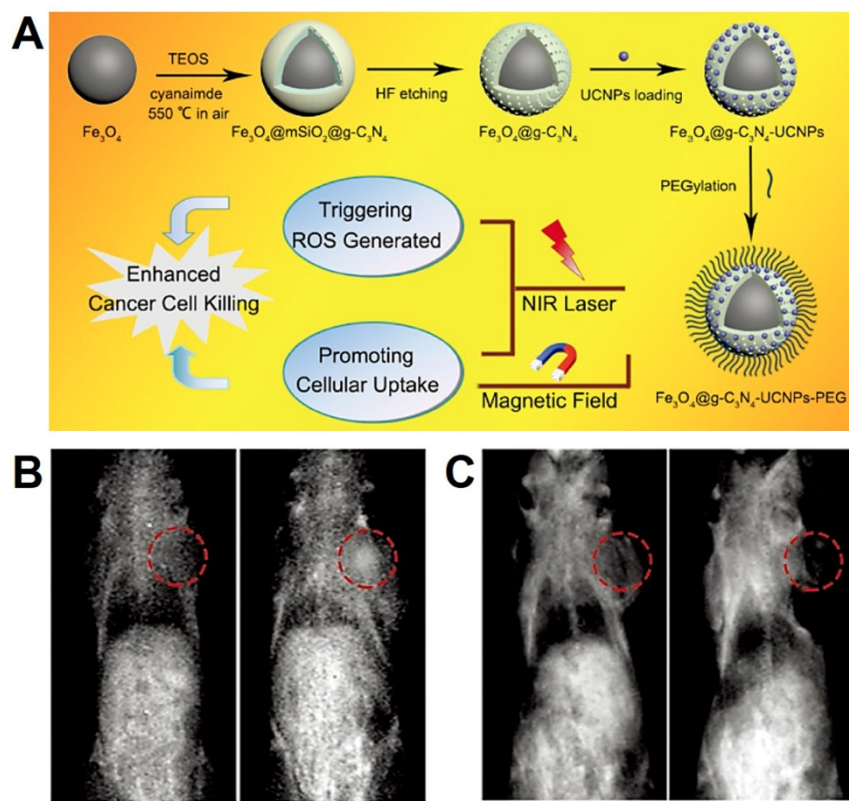
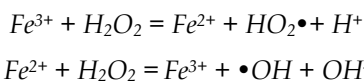


Figure 12. (A) The schematic diagram of synthesis process of $\text{Fe}_3\text{O}_4@g\text{-C}_3\text{N}_4\text{-UCNPs-PEG}$. (B,C) *In vivo* T_2/T_1 -weighted MRI of samples, preinjected and after injection *in situ*. Adapted with permission from [200], copyright 2017 Advanced Healthcare Materials.

5. Fe₃O₄ NPs for Imaging-Guided Tumor Treatment

5.1 Nanozyme

In recent years, Fe₃O₄ NPs are reported to have the intrinsic biocatalytic activity akin to horseradish peroxidase (HRP) [201]. Therefore, inorganic nanoparticles have been used as nanozyme for specific biomedical applications [202, 203]. The mechanism of Fe₃O₄ as nanozyme in killing tumor cells can be understood as the Fenton reaction, which utilizes Fe³⁺/Fe²⁺ ions reaction with excessive H₂O₂ in tumor tissues to generate excessive reactive oxygen species (ROS) [204-206]:



Due to the chain reaction between Fe₃O₄ (Fe²⁺, Fe³⁺) and H₂O₂, the Fenton reaction consumes the H₂O₂ in the tumor tissues and produce the •OH with cytotoxicity [207]. Based on the excellent enzyme-like activities, Fe₃O₄ NPs have been developed as enzyme mimetics for many novel biomedical applications [201]. It is worth mentioning that the efficient Fenton reaction usually require specific conditions, such as lower pH (3.0 ~ 4.0), higher temperature or UV/vis light irradiation. However, the pH value of tumor microenvironment is around 5.5-6.5, which cannot achieve the optimal Fenton reaction conditions [208]. Therefore, for achieve the best therapeutic effect, the

UV/vis light or thermotherapy are always used to assist the Fenton reaction to enhance the ability of producing •OH [209].

Gu *et al.* [210] verified the enzyme-like activities of Fe₃O₄ NPs on role position and pH values. When the Fe₃O₄ NPs were internalized into tumor cells mainly concentrated in lysosomes and the cytotoxicity is related to the concentration. Fe₃O₄ show stronger toxic potency than γ-Fe₂O₃. Due to the acidic microenvironment of lysosomes, Fe₃O₄ NPs presented the peroxidase-like activity and the cell damage would be enhanced by the induced H₂O₂. In neutral pH conditions, both Fe₃O₄ and γ-Fe₂O₃ NPs cannot produce hydroxyl radicals (•OH), but just catalyze decomposition of H₂O₂ into H₂O and O₂ directly. These results show that the cytotoxicity of Fe₃O₄ nanozyme are decided by the external environment and distribution intracellular. Lin *et al.* [211] reported a strategy for enhanced the chemodynamic therapy (CDT) effect by the synergistic of photothermal therapy, which combined the typical Fe₃O₄ nanozyme and the semiconductor Bi₂S₃ as shown in Figure 13A. The Fe₃O₄@Bi₂S₃ nanocatalysts could kill the cancer cells through the effect of photothermal treatment under 808 nm laser, and sequential thermal effect enhanced the Fenton action of Fe₃O₄ NPs, which could efficiently convert H₂O₂ into highly toxic •OH, thus realizing a remarkable synergistic anticancer achievement.

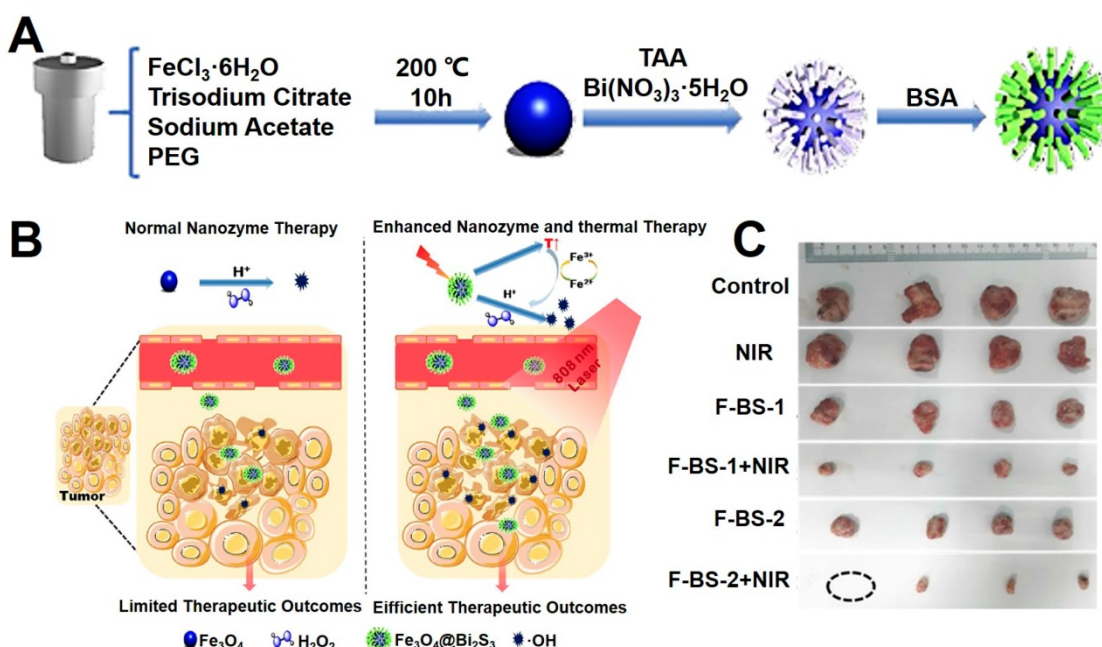


Figure 13. (A) The synthesis mechanism diagram of Fe₃O₄@Bi₂S₃ nanocatalysts. (B) The schematic diagram of *in vivo* photothermal and chemodynamic therapy. (C) The photographs of anatomical tumors *in vivo* of treating groups. Adapted with permission from [211], copyright 2020 ACS Applied Materials & Interfaces.

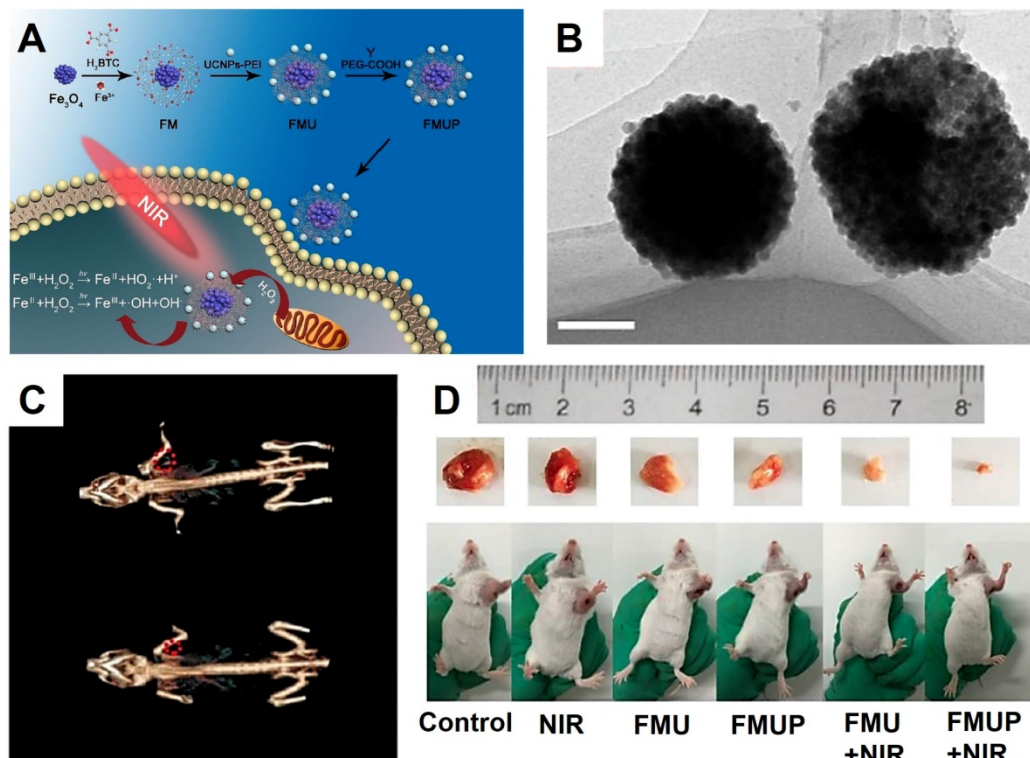


Figure 14. The synthesis process illustration (A) and the TEM images (B) of FMUP (Scale bars: 100 nm). (C) *In vivo* CT images of FMUP before (down) and after injection (up). (D) The photographs of tumor-bearing mice after 14 days of treatment. Adapted with permission from [209], copyright 2018 Chemical Engineering Journal.

Yang *et al.* [209] designed a novel diagnosis and treatment platform composed of Fe_3O_4 NPs, metal organic frame MIL-100(Fe), UCNPs ($\text{NaYF}_4:\text{Yb}, \text{Tm}@\text{NaGdF}_4:\text{Yb}$) and modified by PEG (aliased as FMUP). The UCNPs were designed for converter the near-infrared light to UV/vis light, which could excite the $\text{Fe}^{3+}/\text{Fe}^{2+}$ ions in the Fe_3O_4 NPs and enhance the effect of photo-Fenton reaction, thus activating the photocatalytic reaction by using MIL-100(Fe) as photosensitizer (Figure 14), which synergy combined photodynamic therapy (PDT) and photochemotherapy (PCT). The Fenton reaction produced cytotoxic reactive oxygen ($\cdot\text{OH}$) with high cytotoxicity independent of the oxygen in the tumor microenvironment. Meanwhile, the Fe_3O_4 NPs and MIL-100(Fe) could form the heterojunctions that markedly inhibited the recombination of electrons and holes, thus effect enhancing the ability of PCT and PDT in producing ROS. The antitumor effect was showed by *in vivo* and *in vitro* assays, the experimental results have indicated that the FMUP with the excellent imaging ability of CT and UCL with positive synergistic treatment effect of PDT and PCT.

5.2 Magnetic hyperthermia treatment

Magnetic nanoparticles (MNPs) provide an effective platform for biomedicine with lots of applications such as MRI, magnetic guidance delivery, magnetic separation, and thermal treatments

[212, 213]. The magnetic hyperthermia treatment (MHT) is a classical therapeutic concept based the principle of cancer cells are more vulnerable than healthy cells when the environment temperatures higher than 41 °C. The thermal effect of MNPs could generate by the external alternating magnetic field (AMF) and define by the specific absorption rate (SAR), which is rate value of energy absorbed per unit mass of the agent when located in radio frequency. The values of SAR are influenced by the morphology and composition of the MHT agent, also be affected by the property of magnetic field such as frequency (f) and amplitude (H). Therefore, for achieving an effect of hyperthermia to tumors, the magnetically mediated hyperthermia nanomaterials must show the high SAR and low (f)/(H) in the low content. Thereinto, the superparamagnetic Fe_3O_4 NPs as the heat mediators *via* an oscillating magnetic field show remarkable superiority, because SAR values of superparamagnetic nanoparticles can be enhanced by increasing either (f) or (H) (or both increase) during the measurements [96]. In general, most studies on the SAR carried out on Fe_3O_4 NPs were prepared by co-precipitation method or sol-gel, the resulting nanoparticles were usually in the size of 20-50 nm. Only few researches of SAR prepared by thermal decomposition methods have reported, because small size Fe_3O_4 NPs usually has a low SAR value [212].

Ishimura *et al.* [214] reported the research of superparamagnetic Fe_3O_4 NPs (SPIONs) clusters for MRI and MHT. Superparamagnetism of Fe_3O_4 NPs only present in the size less than 10 nm. However, this size is smaller than capillaries pores of normal tissues and will lead to the leakage of SPIONs from the normal tissues, resulting the low accumulation in tumors, and reduce the effect of the tumor diagnosis and treatment. To obtain effective accumulation and excellent therapeutic effect of magnetic hyperthermia treatment, the FA and PEG modified SPIONs nanoclusters were designed (FA-PEG-SPION NCs). The SPIONs clusters not only prevented the leakage from normal tissues capillaries, but also increased the rate of relaxivity and the specific absorption. Meanwhile, the FA and PEG could also increase the targeting of SPIONs clusters and enhance the amount accumulation in tumors. After intravenous injection the FA-PEG-SPION NCs for 24 h, the clusters would accumulate locally in cancer (not necrotic) tissues and

enhance the MRI intensity. Furthermore, the FA-PEG-SPION showed excellence magnetic hyperthermia effect under the alternating current magnetic field ($f = 230 \text{ kHz}$, $H = 8 \text{ kA/m}$).

Liang *et al.* [215] designed a multifunctional system consisting of Pd modified Fe_3O_4 nanoparticles (JNPs) with the property of dual-mode MRI and PA (photoacoustic) imaging, synergy of photothermal therapy, magnetic therapy and chemodynamic therapy (Figure 15). The plasmonic photothermal property of Pd nanosheets could achieve synergistic effects for enhancing the magnetic/photothermal effect of Fe_3O_4 NPs, and the chemodynamic therapy could be attributed to the $\cdot\text{OH}$, which generate from the Fenton reaction of Fe_3O_4 NPs and catalytic properties of Pd nanosheet in an acidic environment of tumor H_2O_2 . Meanwhile, the ability of reactive oxygen species production could also be further enhanced under alternating magnetic field and near-infrared light irradiation.

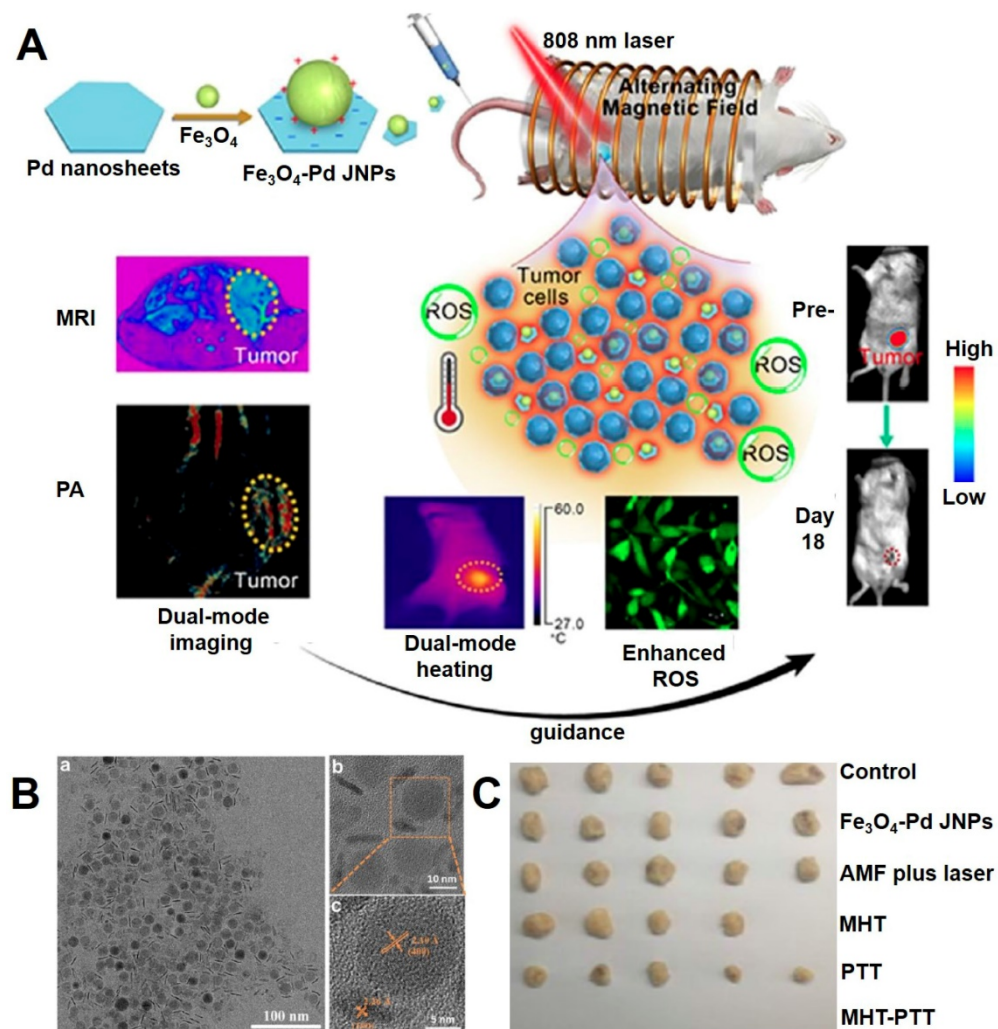


Figure 15. (A) The illustration of the design Fe_3O_4 -Pd JNPs. (B) TEM images of Fe_3O_4 -Pd JNPs (TEM (a), enlarged TEM (b) and HRTEM (c)). (C) The photos of tumor tissues harvested from mice at the end of treatment. Adapted with permission from [215], copyright 2019 Nanoscale Horizons.

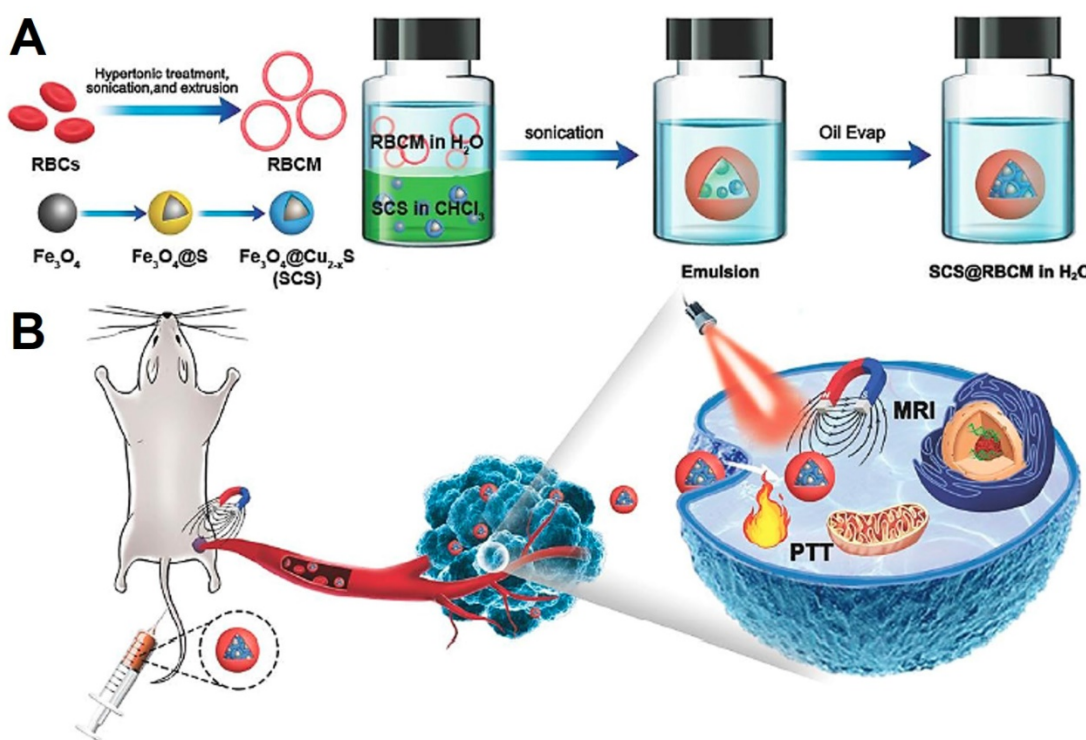


Figure 16. Schematic illustration showing the synthesis process of red blood cell membrane coated $\text{Fe}_3\text{O}_4@\text{Cu}_{2-x}\text{S}$ nanocluster system (A) and magnetic field triggered active targeting of MRI and PTT (B). Adapted with permission from [222], copyright 2020 Journal of Materials Chemistry B.

5.3 Photothermal therapy

Photothermal therapy (PTT) is widely used for tumor therapy in recent years, relying on the nanoparticles in tumor tissues to convert optical energy into thermal energy to kill cancer cells [216]. Compared with surgical management and radiotherapy chemotherapy, PTT is more controllable, highly efficient and lower invasive [217]. This treatment takes the advantage of near-infrared light (NIR) with excellent tissue penetration effect and minimum damage in the range of 700-1100 nm, which could activate specific materials to transformation energy generate thermal effect and cause damage to the tumor tissues. Many nanomaterials have been developed as PTT agents, such as noble metals, semiconductors, and special polymers, which usually have a strong optical absorbance in the near-infrared optical window [218]. The potential toxicity caused by photothermal agents is still an unresolved problem because these nanoparticles tend to accumulate in organs and the slow degradability of nanomaterials would introduce inflammatory cytokine production, increase oxidative stress and cell death, which would limit the clinical application of PTT [219, 220]. Therefore, that necessary to explore the agent with biosafe and biodegradable for PTT.

Fe_3O_4 NPs have been attention due to the excellent biocompatibility, nontoxicity, MRI and magnetic targeting capability [221]. Although the

Fe_3O_4 have been approved as drugs for clinical. However, there are few reports about Fe_3O_4 NPs in photothermal therapy, due to the low molar extinction coefficient and poor photothermal conversion efficiency [222]. In order to improve the photothermal therapy effect of Fe_3O_4 NPs, much research has been done, one common way is to decorate the materials with high photothermal conversion (e.g., noble metals, copper chalcogenides, special polymer) onto the surface of magnetic Fe_3O_4 NPs to enhance the plasma resonance, another is to change the morphology of Fe_3O_4 NPs for obtaining better photothermal conversion effect [223]. Shi *et al.* [224] reported the photothermal effect of special shape magnetic Fe_3O_4 NPs both *in vitro* and *in vivo* experiments. The heating effect of Fe_3O_4 NPs with the shape of spherical, hexagonal and wire-like were found rapidly generated under the red and near-infrared range laser irradiation, which showed obviously damaged on cancer cell cellular organelles. Due to the photothermal effect of the special-shaped Fe_3O_4 NPs, the tumor cells were found to be significant apoptosis with tumor reduction.

Wu *et al.* [222] proposed a simple method to transfer hydrophobic $\text{Fe}_3\text{O}_4@\text{Cu}_{2-x}\text{S}$ NPs to hydrophilic with the help of red blood cell membrane (Figure 16), which showed excellent performance for T_2 -weighted MRI and PTT. The obtained nanoplatform was consist of the densely $\text{Fe}_3\text{O}_4@\text{Cu}_{2-x}\text{S}$

nanocluster core and the red blood cell membrane layer shell. This system displayed a stable nanostructure, excellent magnetic targeting ability and photothermal conversion ability. With the advantages of the red blood cell membrane, the nanocluster was protected from the elimination by macrophages, and showed excellent magnetic targeting under the external magnetic field. Therefore, all of these features promote the platform with high performance for MRI and PTT.

Recent researches have demonstrated the magnetic moment could significantly enhance with the agglomeration state [225]. Therefore, change the monodisperse magnetic Fe_3O_4 NPs into clusters provided an effective way to enhance the specific absorption rate (SAR) [226]. Yang *et al.* [227] reported an efficient PTT platform by self-assembly the monodisperse Fe_3O_4 nanocrystal into spherical superparticles (SPs), which could significantly increase the effect of photothermal treatment (Figure 17). For further enhance the tumor treatment effect, mPEG-PLGA copolymer were used to modify the Fe_3O_4 SPs, and immune adjuvant R837 were loaded to

generate the antigens associated to tumor and induce strong antitumor immune responses synergistic treatment of tumor.

5.4 Photodynamic therapy

Photodynamic therapy (PDT) is considered as an emerging therapeutic strategy for clinical anticancer in recent years, due to the low systemic toxicity, cooperativity and negligible side effects. It includes three important parts: photosensitizers (PS), exciting light and oxygen in the tissue [200]. The principle of PDT is to trigger the reactive oxygen species (ROS) with cytotoxicity to induce tumor cells death. Meanwhile, the accurate delivery of photosensitizer to tumor tissue also play an important part of the treatment process. Magnetic targeting is a classic targeting approach, which takes the advantages of magnetic nanoparticles with the capability of being magnetized and directional movement by an external magnetic field, finally guidance the magnetic nanoparticles concentrate in specific location. This physical interaction exhibiting potential application for tumor targeting, and as an excellent magnetic

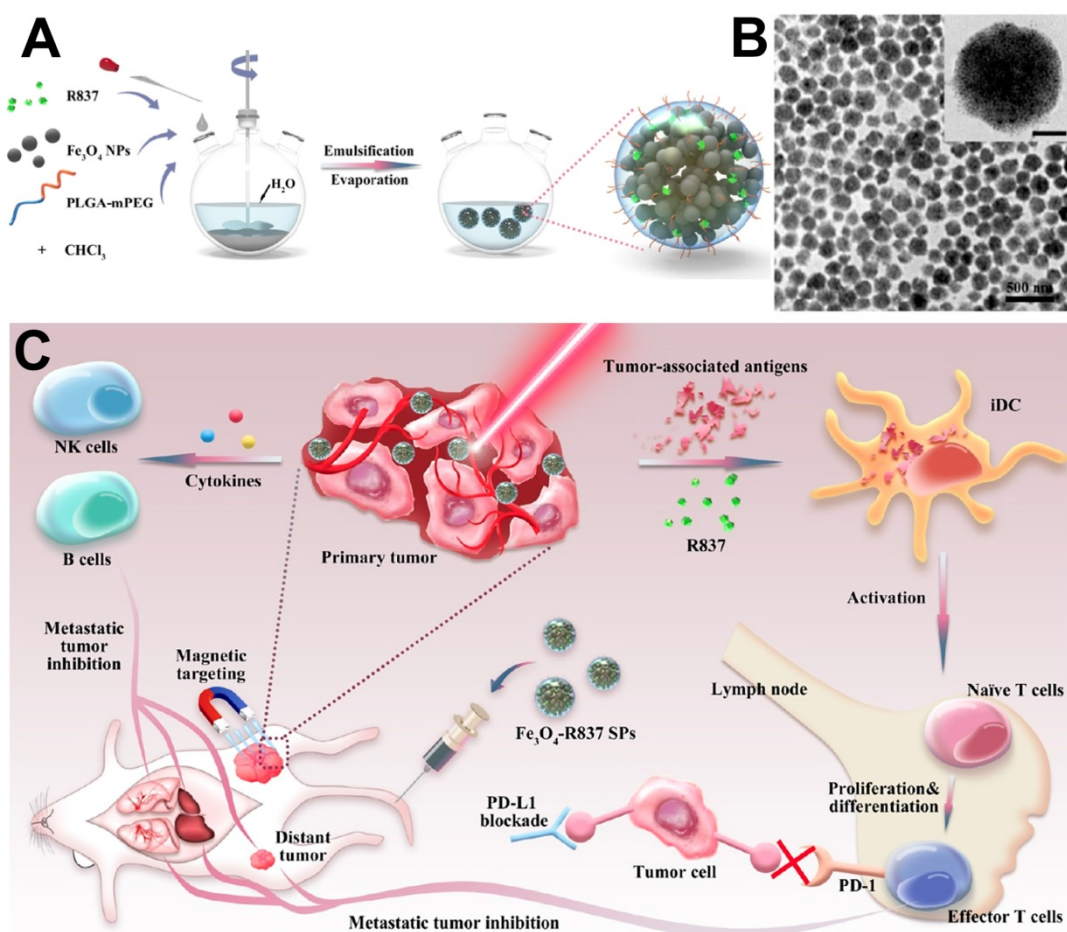


Figure 17. (A) The schematic illustrates of the Fe_3O_4 -R837 SPs synthesis process. (B) TEM images of Fe_3O_4 -R837 SPs (scale bar: 50 nm). (C) The schematic diagram of Fe_3O_4 -R837 SPs for cancer therapy by antitumor immune responses synergistic photothermal therapy. Adapted with permission from [227], copyright 2018 ACS applied materials & interfaces.

carrier, the Fe_3O_4 NPs have been concerns on the excellent MRI performance, magnetic targeted ability, high biocompatibility and chemical stability. Therefore, the effective combination of photosensitizer with Fe_3O_4 NPs could construct the photodynamic therapy nanoplateform with the magnetic targeted and MRI guided.

Lin et al. [228] synthesized a multifunctional treatment platform by covalently grafting Fe_3O_4 on the surface of MoS_2 , then the photosensitizers indocyanine green (ICG) molecules and prodrugs Pt (IV) were loaded on the surface of $\text{MoS}_2@\text{Fe}_3\text{O}_4$ as shown in Figure 18A ($\text{Mo}@\text{Fe-ICG/Pt}$). The high transverse relaxivity Fe_3O_4 NPs in the $\text{Mo}@\text{Fe-ICG/Pt}$ nanocomposites were used as an effectively T_2 -weighted MRI contrast agent, which provided an excellent positioning effect for photothermal therapy of MoS_2 , photodynamic therapy of ICG, and chemotherapy triggered of Pt (IV) prodrugs, thus leading to an ideal nanoplateform for tumor imaging and treatment.

Zhu et al. [229] designed a multifunctional tumor treatment platform composed of Fe_3O_4 core and two kinds of shells, which are MnO_2 and polypyrrole (PPy) as shown in Figure 19. The PPy was used as the agent of photothermal and photosensitizer, then combined with $\text{Fe}_3\text{O}_4@\text{MnO}_2$ for achieving the

magnetic targeting effects. The MnO_2 shell could catalyze the H_2O_2 in the tumor tissues decompose into O_2 to improve the production of ROS under the irradiation, finally enhance the therapeutic effect of PTT/PDT. Meanwhile, the $\text{Fe}_3\text{O}_4@\text{MnO}_2@\text{PPy}$ nanocomposite could also load DOX efficient and implement an acid response release in tumor tissues, which also realized the synergistic chemotherapy and PDT/PTT by avoiding damage to normal cells.

5.5 Chemotherapy drug delivery

The most common non-surgery methods for cancer treatment are chemotherapy and radiation therapy. Nowadays, there are about 80 different kinds of antitumor drugs in the clinic, and around 400 drugs are being tested in clinical trials [230, 231]. Although they are effective in some cancer types, most of them lack specificity towards tumor cells [232]. The normal tissues and organs will be harmed at therapeutic dosage [233]. Tumor-targeting therapy is delivering some chemotherapy drugs or other antitumor bioactive compounds to cancer cells by specific carriers, with limited influence on normal healthy tissues, resulting in higher therapeutic efficiency and lower toxicity [234, 235]. Meanwhile, the target delivery can be classified into three types based on the destination of the drugs, the primary target is

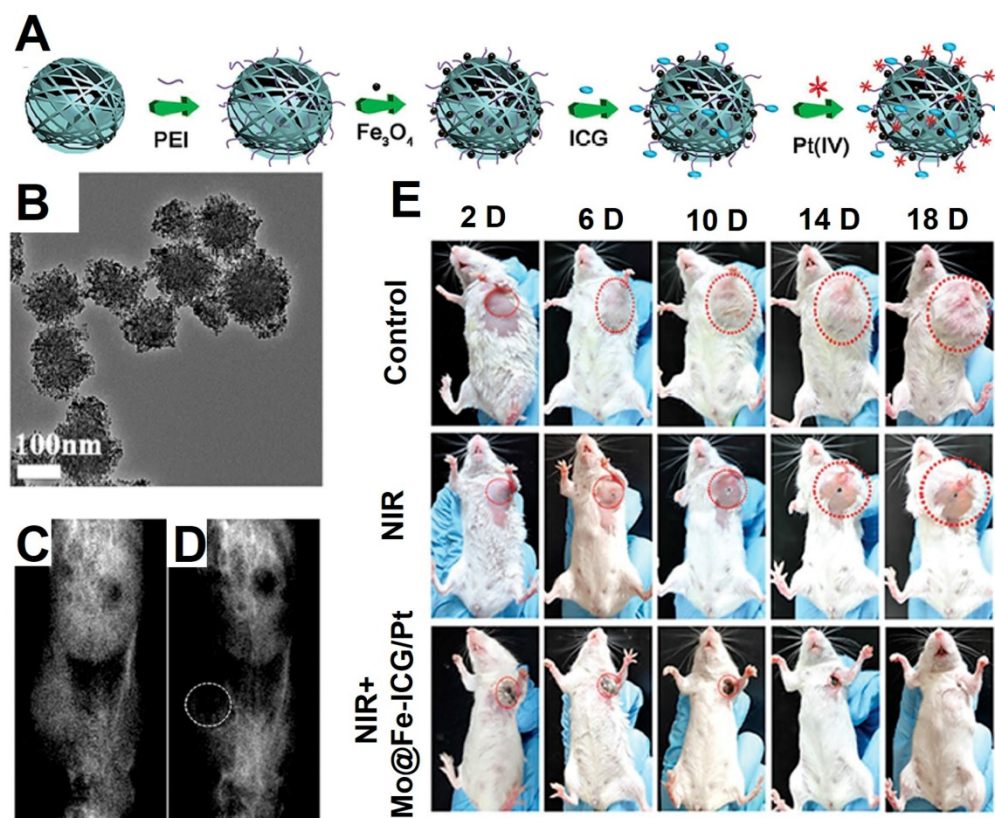


Figure 18. The schematic diagram of the synthesis process (A) and TEM images (B) of $\text{Mo}@\text{Fe-ICG/Pt}$ nanocomposites. The T_2 -weighted MRI preinjection (C) and after injection (D) of $\text{Mo}@\text{Fe-ICG}$. (E) The photographs of mice after treatments by $\text{Mo}@\text{Fe-ICG/Pt}$. Adapted with permission from [228], copyright 2017 Advanced Science.

reaching determined tissues or organs. The secondary target is reaching specific cells. The third-level target is interacting with some specific targets inside cells [236, 237]. So far, tumor nano-delivery systems have attracted main attention on the size so that the drug could enrich in tumor tissues owing to the EPR effect of tumor tissues [238, 239]. Meanwhile, the nano-delivery system could conjugate with some certain ligands to permits the active targeting into tumor tissues. Achieving highly specific targeting to cancer cells is the ultimate goal in cancer therapy and

diagnosis [240, 241].

In 1960s, Freeman *et al* has introduced the magnetically Fe_3O_4 NPs guided anti-cancer drugs delivery carrier is a unique method to concentrate drug accumulation of therapeutic nanoparticles to tumor tissues to improve therapeutic efficacy and used for the MRI contrast agent in 1985s [75, 242]. Meanwhile, the monitoring of drug release *in vivo* provides the accurate and reliable information for guiding the chemotherapy. The *in vivo* drug delivery based on the imaging guiding shows unique

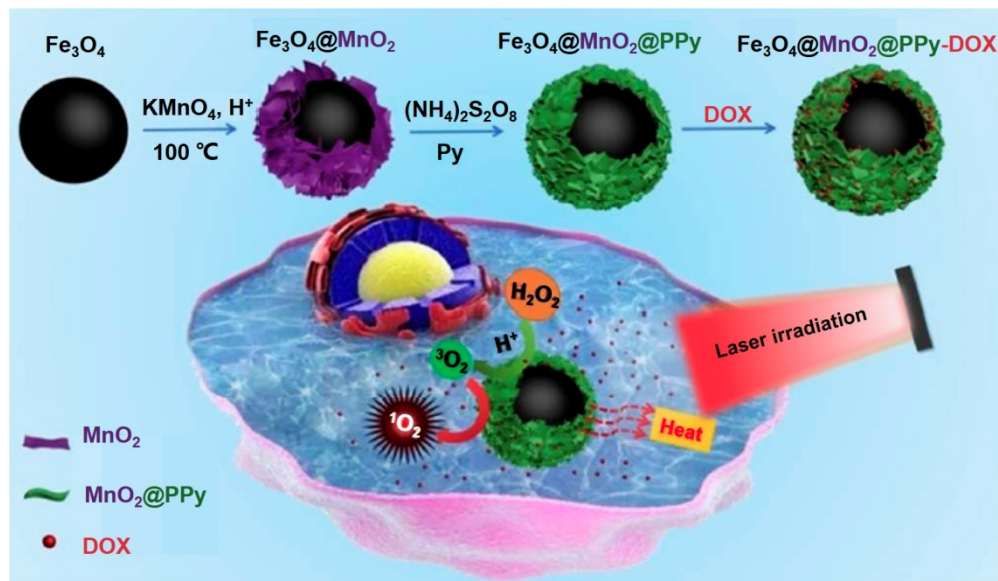


Figure 19. Schematic illustration for the fabrication and magnetic targeting, improved PDT by the catalytic decomposition of H_2O_2 and synergistic chemotherapy and PDT/PTT treatments of the $\text{Fe}_3\text{O}_4@\text{MnO}_2@\text{PPy-DOX}$ to cancer cells. Adapted with permission from [229], copyright 2018 Journal of Materials Chemistry B.

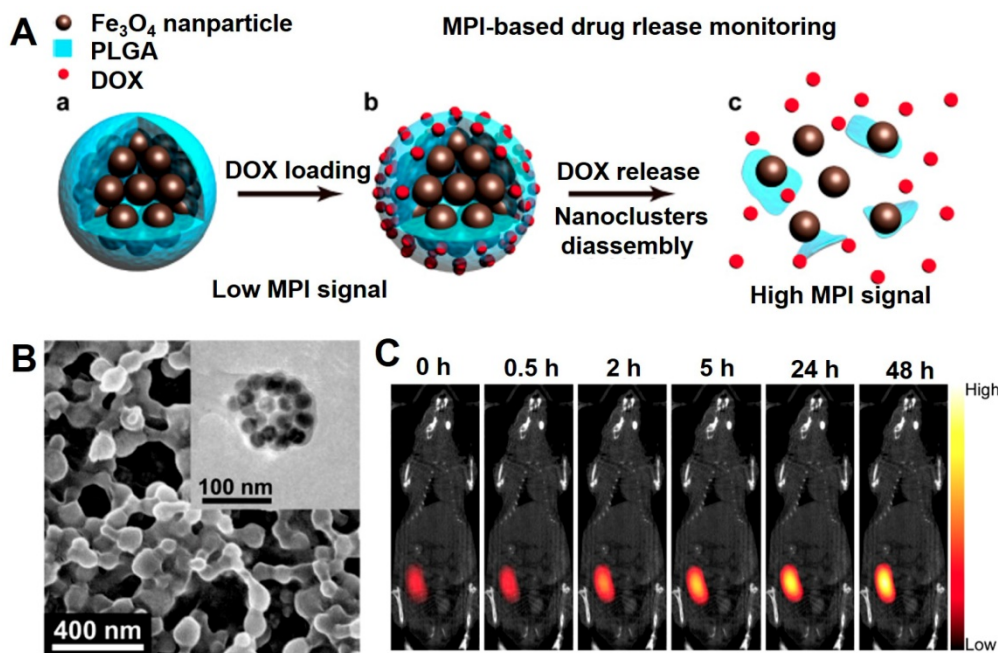


Figure 20. The schematic diagram of $\text{Fe}_3\text{O}_4@\text{PLGA}$ nanocomposite for MPI-based drug release monitoring. (B) SEM image of DOX loaded $\text{Fe}_3\text{O}_4@\text{PLGA}$ nanocomposites, and TEM image of a $\text{Fe}_3\text{O}_4@\text{PLGA}$ nanocomposites (Inset). (C) MPI and CT merged images injected intratumorally with $\text{Fe}_3\text{O}_4@\text{PLGA}$. Adapted with permission from [243], copyright 2019 Nano letters.

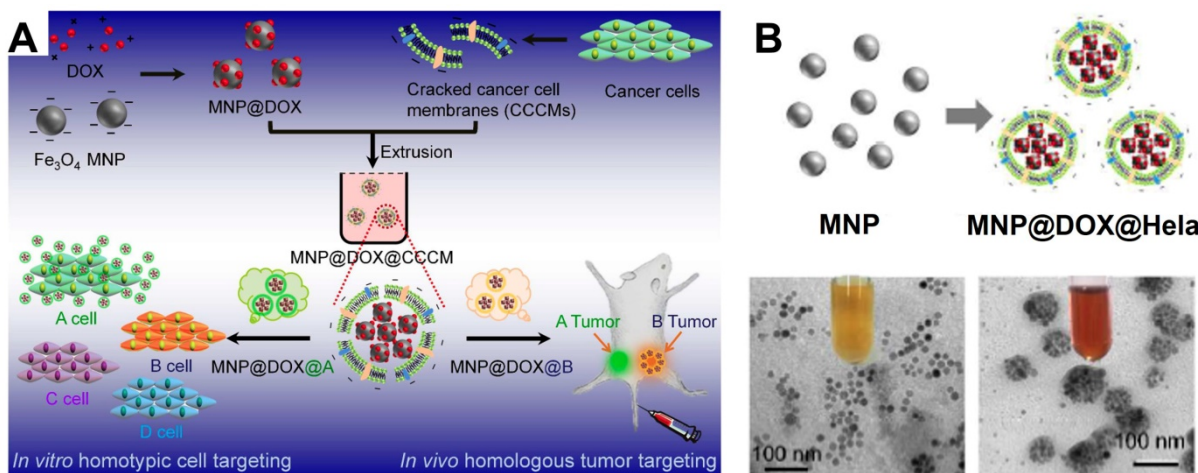


Figure 21. (A) The schematic diagram of cracked cancer cell membrane (CCCM) embellished MNPs and the mechanism for prioritizing cancer cells recognition; (B) TEM images of MNP and MNP@DOX@CCCM. Adapted with permission from [250], copyright 2016 Nano Letters.

advantageous due to the no invasiveness and the drug distribution visualization [243]. Magnetic particle imaging (MPI) due to the deeper tissue penetration and quantifiable signal intensity are widely used in detecting drug release *in vivo*, which mainly use the superparamagnetic Fe₃O₄ NPs as the contrast agent and sole signal source [244, 245]. Smith *et al.* [243] designed a core-shell nanocomposite consisting of the superparamagnetic Fe₃O₄ nanocluster and PLGA loaded with the chemotherapy drug DOX, which could be applied for drug delivery and the tracer of MPI quantification (Figure 20). The core-shell nanocomposite can occur decomposition in the tumor microenvironment (pH = 6.5), which could induce the gradual decomposition of the Fe₃O₄ nanocluster, sustained release of DOX and the change of MPI signal. The results indicated that induced MPI signal changes and the release rate of DOX over time displayed a linear correlation ($R^2 = 0.99$). Using this phenomenon, the chemotherapy drug release process in tumor tissue can be successfully monitored to assess the induced tumor cell damage.

In recent years, the delivery of drug using cancer cell membrane, especially that from the homologous tumors has become an emerging tumor-targeting modification method [246]. In this context, a series of cancer cell membrane modified Fe₃O₄ NPs for the cancer diagnosis and treatment are reported. By modifying employ the source cancer cell membrane *in vitro*, the Fe₃O₄ NPs are identified with the self-recognition internalization, and “homing” targeting ability to the homologous tumor *in vivo* to precisely deliver the drugs to the appropriate tumor sites [247, 248]. As a result, Fe₃O₄-based delivery system shows strong curative effect for MRI and tumor treatment *in vivo*. This delivery strategy by modifying cell membrane on the traditional delivery

system have shown great potentials for precise targeting to particular tumors by merely adjusting the corresponding type of modified cell membrane [249, 250]. Zhang *et al.* [250] devised a magnetic Fe₃O₄ NPs (MNP) based diagnosis and treatment nanomaterials platform, and modified the cracked cancer cell membranes (CCCM) on the surface coating the Fe₃O₄ NPs with the particular kind of cell membrane derived from a specific delivery system to correspond type of tumor (Figure 21). Meanwhile, the chemotherapy drug DOX can also be delivered with the CCCM modified MNP system, which showed self-recognition to the same cancer cell lines by the “homing” to the homologous tumor *in vivo*. These results provide a new approach to develop highly tumor-recognizing self-targeting nanosystems for cancer therapy and diagnosis.

5.6 Gene delivery

Small interfering RNA (siRNA) could downregulate specific protein expression by suppressing a targeted gene selectively at the mRNA transcription level through a mechanism called RNA interference (RNAi) [251, 252], which have been widely researched for treating a variety of genetic diseases, such as cardiovascular diseases and cancers [253, 254]. Despite of these advantages, the low transport efficiency of siRNA with severe side effects still limits the clinical use [255, 256]. Fe₃O₄ NPs are well-established depend on possess magnetic properties, actively investigated as new generation for MRI, excellent biocompatibility and versatile surface functionalization capability, due to the unique characteristics, Fe₃O₄ NPs are extensively explored for various biomedical applications especially in delivery of therapeutics, antibodies, peptides, nucleic acids, and other assorted biological agents biological agents

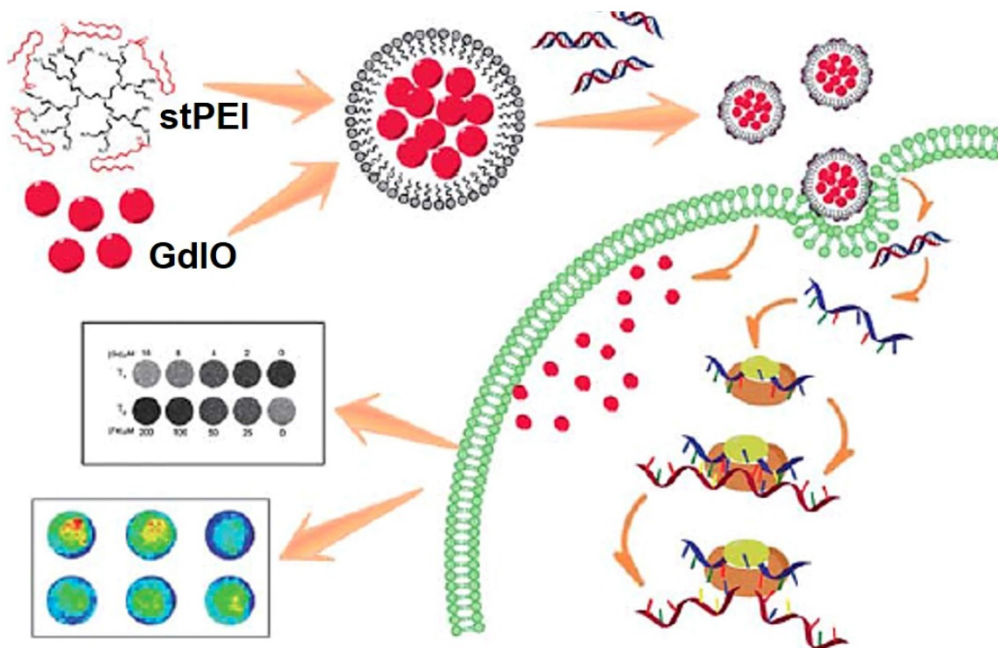


Figure 22. Schematic illustration of the preparation of GdIO-stPEI/siRNA complexes and their function. Adapted with permission from [259], copyright 2013 Nanoscale.

[257, 258]. Chen *et al.* [259] reported a multifunctional nanoclusters as an agent for dual-modal T_1 - T_2 MRI imaging and siRNA delivery (Figure 22). The hydrophilic nanoclusters were self-assembled from the hydrophobic gadolinium (Gd) embedded Fe_3O_4 nanocrystals (GdIO), after self-assembly with polyethylenimine (stPEI), the obtained GdIO-stPEI nanoclusters showed good stability, dispersity and dual-modal T_1 - T_2 -weight MRI properties. Meanwhile, the composite nanoclusters with the ability to deliver the siRNA, while maintaining other properties such as magnetism, biocompatibility, and imaging performance, thus providing a safe and efficient method for imaging guidance gene delivery.

Conclusion and Perspective

In summary, we reviewed the recent research of Fe_3O_4 NPs from the synthesis, surface modification, and focus description the novel biomedical applications in tumor imaging and therapy. With the development of nanotechnology more high quality Fe_3O_4 NPs synthesis methods are reported, and the surface modification of Fe_3O_4 NPs also became more functional. New-generation Fe_3O_4 -based contrast agents could realize the multimode and responsive imaging, provided more accurate and effective information for tumor diagnosis and guided follow treatment.

At present, the clinical application of multifunctional Fe_3O_4 is mainly in MRI contrast agent, not really implemented the integration of diagnosis and treatment [260]. First, the complex preparation

process, high cost and long tumor treatment trial period limit the clinical use of Fe_3O_4 -based drugs. Second, although the magnetic targeting could increase the accumulation of Fe_3O_4 -based drugs in tumor tissues, the available percentage still less than 2 % of the intravenously administrated dose. Third, there may be no EPR effect of the nanomaterials in the solid tumor of human beings comparing with the nude mouse tumor models. Last but not the least important, the potential toxicity of nanoparticles has not been properly addressed. Totally, these disadvantages limit the Fe_3O_4 -based drugs for the further clinical applications. We believe these advanced reports will guide the academic researchers and industries to accurate the present translational stage for the further bioapplications utilized with these multifunctionalized magnetic iron oxide nanomaterials.

Abbreviations

- multifunctional magnetic nanoparticles (MNPs)
- magnetic iron oxide (Fe_3O_4)
- nanoparticles (NPs)
- enhanced permeation and retention (EPR)
- superparamagnetic iron oxide nanoparticles (SPIONs)
- magnetic resonance imaging (MRI)
- tumor microenvironment (TME)
- gadolinium (Gd)
- metal-organic frameworks (MOF)
- polyvinylpyrrolidone (PVP)
- polyethylene glycol (PEG)

polyethyleneimine (PEI)
 Oleic acid (OA)
 1-octadecene (ODE)
 oleylamine (OAm)
 poly (lactic-coglycolicacid) (PLGA)
 polystyrene (PS)
 polyacrylicacid (PAA)
 tetrahydrofuran (THF)
 3-mercaptopropyl trimethoxysilane (MPTMS)
 poly(L-lysine) (PLL)
 poly(propyleneimine) (PPI)
 poly(glycerol succinic acid) (PGLOSAOH)
 poly (vinyl alcohol) (PVA)
 microcapsules (MCs)
 premix membrane emulsification (PME)
 platelet (PLT)
 near infrared (NIR)
 photothermal therapy (PTT)
 systematic evolution of ligands by exponential enrichment (SELEX)
 doxorubicin (DOX)
 alginate nanogels (AG NGs)
 polyethyleneimine (PEI)
 phosphine oxide (PO)
 upconversion nanoparticles (UCNPs)
 horseradish peroxidase (HRP)
 reactive oxygen species (ROS)
 photochemotherapy (PCT)
 near-infrared (NIR)
 photodynamic therapy (PDT)
 computed tomography (CT)
 upconversion luminescence imaging (UCL)
 photosensitizers (PS)
 singlet oxygen (${}^1\text{O}_2$)
 indocyanine green (ICG)
 magnetic hyperthermia treatment (MHT)
 specific absorption rate (SAR)
 superparticles (SPs)
 oil-in-water (O/W)
 dendritic cells (DCs)
 draining lymph nodes (DLNs)
 cracked cancer cell membranes (CCCM)
 small interfering RNA (siRNA)
 RNA interference (RNAi)
 gadolinium embedded iron oxide (GdIO)
 stearic acid modified low molecular weight polyethylenimine (stPEI)

Acknowledgements

This work was supported by National Natural Science Foundation of China (31800833, 21977081), Zhejiang Provincial Natural Science Foundation of China (Z19H180001), Wenzhou Medical University (89218028, KYYW201901), Wenzhou Institute of Biomaterials & Engineering (WIBEZD2017001-03),

University of Chinese Academy of Science (WIUCASYJ2020001), the Wenzhou Science and Technology Plan Project (ZY202005) and Wenzhou Science and Technology Plan Project (Y20180071).

Competing Interests

The authors have declared that no competing interest exists.

References

- Elsherbiny IM, Elbaz NM, Sedki M, Elgammal A, Yacoub MH. Magnetic nanoparticles-based drug and gene delivery systems for the treatment of pulmonary diseases. *Nanomedicine*. 2017; 12: 387-402.
- Yen SK, Padmanabhan P, Selvan ST. Multifunctional iron oxide nanoparticles for diagnostics, therapy and macromolecule delivery. *Theranostics*. 2013; 3: 986-1003.
- Ni J, Li Y, Yue W, Liu B, Li K. Nanoparticle-based cell trackers for biomedical applications. *Theranostics*. 2020; 10: 1923-47.
- Pradhan L, Thakur B, Srivastava R, Ray P, Bahadur D. Assessing therapeutic potential of magnetic mesoporous nanoassemblies for chemo-resistant tumors. *Theranostics*. 2016; 6: 1557-72.
- Ke H, Wang J, Tong S, Jin Y, Wang S, Qu E, et al. Gold nanoshelled liquid perfluorocarbon magnetic nanocapsules: a nanotheranostic platform for bimodal ultrasound/magnetic resonance imaging guided photothermal tumor ablation. *Theranostics*. 2014; 4: 12-23.
- Chinen AB, Guan CM, Ferrer JR, Barnaby SN, Merkel TJ, Mirkin CA. Nanoparticle probes for the detection of cancer biomarkers, cells, and tissues by fluorescence. *Chem Rev*. 2015; 115: 10530-74.
- Li S, Xu L, Ma W, Wu X, Sun M, Kuang H, et al. Dual-mode ultrasensitive quantification of microRNA in living cells by chiroplasmonic nanopyramids self-assembled from gold and upconversion nanoparticles. *Journal of the American Chemical Society*. 2015; 138: 306-12.
- Sun M, Xu L, Ma W, Wu X, Kuang H, Wang L, et al. Hierarchical plasmonic nanorods and upconversion core-satellite nanoassemblies for multimodal imaging-guided combination phototherapy. *Adv Mater*. 2016; 28: 898-904.
- Caraciolo G, Farokhzad OC, Mahmoudi M. Biological identity of nanoparticles *in vivo*: clinical implications of the protein corona. *Trends Biotechnol*. 2017; 35: 257-64.
- Li J, Rao J, Pu K. Recent progress on semiconducting polymer nanoparticles for molecular imaging and cancer phototherapy. *Biomaterials*. 2018; 155: 217-35.
- Yoon HY, Selvan ST, Yang Y, Kim MJ, Yi DK, Kwon IC, et al. Engineering nanoparticle strategies for effective cancer immunotherapy. *Biomaterials*. 2018; 178: 597-607.
- Shen J, Zhang W, Qi R, Mao Z, Shen H. Engineering functional inorganic-organic hybrid systems: advances in siRNA therapeutics. *Chem Soc Rev*. 2018; 47: 1969-95.
- Satpathy M, Wang L, Zielinski R, Qian W, Wang YA, Mohs AM, et al. Targeted drug delivery and image-guided therapy of heterogeneous ovarian cancer using HER2-targeted theranostic nanoparticles. *Theranostics*. 2019; 9: 778-95.
- Nicolas J, Mura S, Brambilla D, Mackiewicz N, Couvreur P. Design, functionalization strategies and biomedical applications of targeted biodegradable/biocompatible polymer-based nanocarriers for drug delivery. *Chem Soc Rev*. 2013; 42: 1147-235.
- Lim E, Kim T, Paik S, Haam S, Huh Y, Lee K. Nanomaterials for Theranostics: Recent Advances and Future Challenges. *Chem Rev*. 2015; 115: 327-94.
- Chen Z, Peng Y, Xie X, Feng Y, Li T, Li S, et al. Dendrimer-Functionalized Superparamagnetic Nanobeacons for Real-Time Detection and Depletion of HSP90α mRNA and MR Imaging. *Theranostics*. 2019; 9: 5784-96.
- Bai J, Wang JT, Rubio N, Protti A, Heidari H, Elgogary RI, et al. Triple-modal imaging of magnetically-targeted nanocapsules in solid tumours *in vivo*. *Theranostics*. 2016; 6: 342-56.
- Kanamala M, Wilson WR, Yang M, Palmer BD, Wu Z. Mechanisms and biomaterials in pH-responsive tumour targeted drug delivery: A review. *Biomaterials*. 2016; 85: 152-67.
- Wang J, Mao W, Lock LL, Tang J, Sui M, Sun W, et al. The role of micelle size in tumor accumulation, penetration, and treatment. *ACS Nano*. 2015; 9: 7195-206.
- Xie W, Guo Z, Gao F, Gao Q, Wang D, Liaw B, et al. Shape-, size- and structure-controlled synthesis and biocompatibility of iron oxide nanoparticles for magnetic theranostics. *Theranostics*. 2018; 8: 3284-307.
- Shen Y, Wu C, Uyeda TQP, Plaza GR, Liu B, Han Y, et al. Elongated nanoparticle aggregates in cancer cells for mechanical destruction with low frequency rotating magnetic field. *Theranostics*. 2017; 7: 1735-48.
- Gilroy KD, Ruditskiy A, Peng H, Qin D, Xia Y. Bimetallic nanocrystals: syntheses, properties, and applications. *Chem Rev*. 2016; 116: 10414-72.
- Lee N, Yoo D, Ling D, Cho MH, Hyeon T, Cheon J. Iron oxide based nanoparticles for multimodal imaging and magnetoresponsive therapy. *Chem Rev*. 2015; 115: 10637-89.

24. Wu M, Yang Y. Metal-organic framework (MOF)-based drug/cargo delivery and cancer therapy. *Adv Mater.* 2017; 29: 1606134.
25. Chandrasekharan P, Tay ZW, Hensley DW, Zhou XY, Fung BK, Colson C, et al. Using magnetic particle imaging systems to localize and guide magnetic hyperthermia treatment: tracers, hardware, and future medical applications. *Theranostics.* 2020; 10: 2965-81.
26. Fan C, Cheng Y, Ting C, Ho Y, Hsu P, Liu H, et al. Ultrasound/magnetic targeting with SPIO-DOX-microparticle complex for image-guided drug delivery in brain tumors. *Theranostics.* 2016; 6: 1542-56.
27. Jin H, Qian Y, Dai Y, Qiao S, Huang C, Lu L, et al. Magnetic enrichment of dendritic cell vaccine in lymph node with fluorescent-magnetic nanoparticles enhanced cancer immunotherapy. *Theranostics.* 2016; 6: 2000-14.
28. Su Y, Fang J, Liao C, Lin C, Li Y, Hu S. Targeted mesoporous iron oxide nanoparticles-encapsulated perfluorohexane and a hydrophobic drug for deep tumor penetration and therapy. *Theranostics.* 2015; 5: 1233-48.
29. Li S, Shang L, Xu B, Wang S, Gu K, Wu Q, et al. A nanozyme with photo-enhanced dual enzyme-like activities for deep pancreatic cancer therapy. *Angew Chem Int Ed Engl.* 2019; 58: 12624-31.
30. Belkahla H, Mazario E, Sangnier AP, Lomas JS, Gharbi T, Ammar S, et al. TRAIL acts synergistically with iron oxide nanocluster-mediated magneto- and photothermal. *Theranostics.* 2019; 9: 5924-36.
31. Curcio A, Silva AKA, Cabana S, Espinosa A, Baptiste B, Menguy N, et al. Iron oxide nanoflowers@CuS Hybrids for Cancer Tri-Therapy: interplay of photothermal therapy, magnetic hyperthermia and photodynamic therapy. *Theranostics.* 2019; 9: 1288-302.
32. Mukherjee S, Sonanini D, Maurer A, Daldruplink HE. The yin and yang of imaging tumor associated macrophages with PET and MRI. *Theranostics.* 2019; 9: 7730-48.
33. Gaubert M, Fournier AP, Docagne F, Vivien D, De Lizarrondo SM. Molecular magnetic resonance imaging of endothelial activation in the central nervous system. *Theranostics.* 2018; 8: 1195-212.
34. Ray S, Li Z, Hsu C, Hwang L, Lin Y, Chou P, et al. Dendrimer- and copolymer-based nanoparticles for magnetic resonance cancer theranostics. *Theranostics.* 2018; 8: 6322-49.
35. Cho IK, Moran S, Paudyal R, Piotrowskanitsche K, Cheng PH, Zhang X, et al. Longitudinal monitoring of stem cell grafts *in vivo* using magnetic resonance imaging with inducible maga as a genetic reporter. *Theranostics.* 2014; 4: 972-89.
36. Karimianjazi K, Munch P, Alexander A, Fischer M, Pfleiderer K, Piechutta M, et al. Monitoring innate immune cell dynamics in the glioma microenvironment by magnetic resonance imaging and multiphoton microscopy (MR-MPM). *Theranostics.* 2020; 10: 1873-83.
37. Jia Z, Song L, Zang F, Song J, Zhang W, Yan C, et al. Active-target T₁-weighted MR Imaging of Tiny Hepatic Tumor via RGD modified ultra-small Fe₃O₄ Nanoprobes. *Theranostics.* 2016; 6: 1780-91.
38. Melemenidis S, Jefferson A, Ruparelia N, Akhtar AM, Xie J, Allen D, et al. Molecular magnetic resonance imaging of angiogenesis *in vivo* using polyvalent cyclic RGD-iron oxide microparticle conjugates. *Theranostics.* 2015; 5: 515-29.
39. Yang Y, Sun Y, Liu Y, Peng J, Wu Y, Zhang Y, et al. Long-term *in vivo* biodistribution and toxicity of Gd(OH)₃ nanorods. *Biomaterials.* 2013; 34: 508-15.
40. Weng Q, Hu X, Zheng J, Xia F, Wang N, Liao H, et al. Toxicological Risk Assessments of Iron Oxide Nanocluster- and Gadolinium-Based T₁ MRI Contrast Agents in Renal Failure Rats. *ACS nano.* 2019; 13: 6801-12.
41. Shen Z, Chen T, Ma X, Ren W, Zhou Z, Zhu G, et al. Multifunctional theranostic nanoparticles based on exceedingly small magnetic iron oxide nanoparticles for T₁-weighted magnetic resonance imaging and chemotherapy. *ACS nano.* 2017; 11: 10992-1004.
42. Sharma SK, Shrivastava N, Rossi F, Tung LD, Thanh NTK. Nanoparticles-based magnetic and photo induced hyperthermia for cancer treatment. *Nano Today.* 2019; 29: 100795.
43. Sang M, Luo R, Bai Y, Dou J, Zhang Z, Liu F, et al. Mitochondrial membrane anchored photosensitive nano-device for lipid hydroperoxides burst and inducing ferroptosis to surmount therapy-resistant cancer. *Theranostics.* 2019; 9: 6209-23.
44. Gobbo OL, Sjaastad K, Radomski MW, Volkov Y, Prinamello A. Magnetic nanoparticles in cancer theranostics. *Theranostics.* 2015; 5: 1249-63.
45. Torti SV, Torti FM. Winning the war with iron. *Nat Nanotechnol.* 2019; 14: 499-500.
46. Ge R, Li X, Lin M, Wang D, Li S, Liu S, et al. Fe₃O₄@polydopamine composite theranostic superparticles employing preassembled Fe₃O₄ nanoparticles as the Core. *ACS Appl Mater Interfaces.* 2016; 8: 22942-52.
47. Hu Y, Zhou Y, Zhao N, Liu F, Xu FJ. Multifunctional pDNA-conjugated polycationic Au nanorod-coated Fe₃O₄ hierarchical nanocomposites for trimodal imaging and combined photothermal/gene therapy. *Small.* 2016; 12: 2459-68.
48. Veiseli O, Gunn JW, Zhang M. Design and fabrication of magnetic nanoparticles for targeted drug delivery and imaging. *Adv Drug Deliv Rev.* 2010; 62: 284-304.
49. Reddy LH, Arias JL, Nicolas J, Couvreur P. Magnetic nanoparticles: design and characterization, toxicity and biocompatibility, pharmaceutical and biomedical applications. *Chem Rev.* 2012; 112: 5818-78.
50. Gao N, Bozeman EN, Qian W, Wang L, Chen H, Lipowska M, et al. Tumor penetrating theranostic nanoparticles for enhancement of targeted and image-guided drug delivery into peritoneal tumors following intraperitoneal delivery. *Theranostics.* 2017; 7: 1689-704.
51. Yang E, Qian W, Cao Z, Wang L, Bozeman EN, Ward C, et al. Theranostic nanoparticles carrying doxorubicin attenuate targeting ligand specific antibody responses following Systemic Delivery. *Theranostics.* 2015; 5: 43-61.
52. Roca A, Costo R, Rebolledo A, Veintemillas-Verdaguer S, Tartaj P, Gonzalez-Carreno T, et al. Progress in the preparation of magnetic nanoparticles for applications in biomedicine. *J Phys D Appl Phys.* 2009; 42: 224002.
53. Latham AH, Williams ME. Controlling transport and chemical functionality of magnetic nanoparticles. *Acc Chem Res.* 2008; 41: 411-20.
54. Kakwani H, Materia ME, Curcio A, Prato M, Sathy A, Nitti S, et al. Dually responsive gold-iron oxide heterodimers: merging stimuli-responsive surface properties with intrinsic inorganic material features. *Nanoscale.* 2018; 10: 3930-44.
55. Arami H, Khandhar A, Liggitt D, Krishnan KM. In vivo delivery, pharmacokinetics, biodistribution and toxicity of iron oxide nanoparticles. *Chem Soc Rev.* 2015; 44: 8576-607.
56. Gobbo OL, Sjaastad K, Radomski MW, Volkov Y, Prina-Mello A. Magnetic nanoparticles in cancer theranostics. *Theranostics.* 2015; 5: 1249-63.
57. Miao P, Tang Y, Wang L. DNA modified Fe₃O₄@Au magnetic nanoparticles as selective probes for simultaneous detection of heavy metal ions. *ACS Appl Mater Interfaces.* 2017; 9: 3940-7.
58. Zhao J, Zhang Z, Xue Y, Wang G, Cheng Y, Pan Y, et al. Anti-tumor macrophages activated by ferumoxytol combined or surface-functionalized with the TLR3 agonist poly (I : C) promote melanoma regression. *Theranostics.* 2018; 8: 6307-21.
59. Ulbrich K, Hola K, Subr V, Bakandritos A, Tucek J, Zboril R. Targeted drug delivery with polymers and magnetic nanoparticles: covalent and noncovalent approaches, release control, and clinical studies. *Chem Rev.* 2016; 116: 5338-431.
60. Ling D, Hyeon T. Chemical design of biocompatible iron oxide nanoparticles for medical applications. *Small.* 2013; 9: 1450-66.
61. Polichetti M, Modestino M, Galluzzi A, Pace S, Iuliano M, Ciambelli P, et al. Influence of citric acid and oleic acid coating on the dc magnetic properties of Fe₃O₄ magnetic nanoparticles. *Mater Today Proc.* 2020; 20: 21-4.
62. Rippe M, Michelas M, Putaux J-L, Fratzl M, Eslava GG, Dempsey NM, et al. Synthesis and magnetic manipulation of hybrid nanobeads based on Fe₃O₄ nanoclusters and hyaluronic acid grafted with an ethylene glycol-based copolymer. *Appl Surf Sci.* 2020; 14534.
63. Belyanina IV, Zamay TN, Zamay GS, Zamay SS, Kolovskaya OS, Ivanchenko TI, et al. In vivo cancer cells elimination guided by aptamer-functionalized gold-coated magnetic nanoparticles and controlled with low frequency alternating magnetic field. *Theranostics.* 2017; 7: 3326-37.
64. Almstatter I, Mykhaylyk O, Settles M, Altomonte J, Aichler M, Walch A, et al. Characterization of magnetic viral complexes for targeted delivery in oncology. *Theranostics.* 2015; 5: 667-85.
65. Huang R, Lin Y, Lin S, Li Y, Chiang C, Chang C. Magnetic ternary nanohybrids for nonviral gene delivery of stem cells and applications on cancer therapy. *Theranostics.* 2019; 9: 2411-23.
66. Liu Z, Lin H, Zhao M, Dai C, Zhang S, Peng W, et al. 2D superparamagnetic tantalum carbide composite MXenes for efficient breast-cancer theranostics. *Theranostics.* 2018; 8: 1648-64.
67. Yu J, Yin W, Zheng X, Tian G, Zhang X, Bao T, et al. Smart MoS₂/Fe₃O₄ nanotheranostic for magnetically targeted photothermal therapy guided by magnetic resonance/photoacoustic imaging. *Theranostics.* 2015; 5: 931-45.
68. Cano I, Martin C, Fernandes JA, Lodge RW, Dupont J, Casado-Carmona FA, et al. Paramagnetic ionic liquid-coated SiO₂@Fe₃O₄ nanoparticles-The next generation of magnetically recoverable nanocatalysts applied in the glycolysis of PET. *Appl Catal B 2020;* 260: 118110.
69. Li C, Liu J, Wang Z, Lv S, Zhao N, Wang S. Integration of Fe₃O₄@UiO-66-NH₂-MON core-shell structured adsorbents for specific preconcentration and sensitive determination of aflatoxins against complex sample matrix. *J Hazard Mater.* 2020; 384: 121348.
70. Natarajan S, Anitha V, Gajula GP, Thiagarajan V. Synthesis and characterization of magnetic superadsorbent Fe₃O₄-PEG-Mg-Al-LDH nanocomposites for ultrahigh removal of organic dyes. *ACS Omega.* 2020.
71. Wang X, Pan F, Xiang Z, Jia W, Lu W. Magnetic Fe₃O₄@PVP nanotubes with high heating efficiency for MRI-guided magnetic hyperthermia applications. *Mater Lett.* 2020; 262: 127187.
72. Wu S, Chen Y, Wang H, Chou M, Chang T, Yuan S, et al. Bispecific antibody conjugated manganese-based magnetic engineered iron oxide for imaging of HER2/neu- and EGFR-expressing tumors. *Theranostics.* 2016; 6: 118-30.
73. Cheng L, Wang C, Feng L, Yang K, Liu Z. Functional nanomaterials for phototherapies of cancer. *Chem Rev.* 2014; 114: 10869-939.
74. Bennett KM, Jo J-i, Cabral H, Bakalova R, Aoki I. MR imaging techniques for nano-pathophysiology and theranostics. *Adv Drug Deliv Rev.* 2014; 74: 75-94.
75. Wu L, Mendoza-Garcia A, Li Q, Sun S. Organic phase syntheses of magnetic nanoparticles and their applications. *Chem Rev.* 2016; 116: 10473-512.
76. Wei H, Wang E. Nanomaterials with enzyme-like characteristics (nanozymes): next-generation artificial enzymes. *Chem Soc Rev.* 2013; 42: 6060-93.
77. Zhang Z, Zhang X, Liu B, Liu J. Molecular imprinting on inorganic nanozymes for hundred-fold enzyme specificity. *Journal of the American Chemical Society.* 2017; 139: 5412-9.

78. Fevre RL, Duranddubief M, Chebbi I, Mandawala C, Valet J, Idbah A, et al. Enhanced antitumor efficacy of biocompatible magnetosomes for the magnetic hyperthermia treatment of glioblastoma. *Theranostics*. 2017; 7: 4618-31.
79. Laurent S, Forge D, Port M, Roch A, Robic C, Vander Elst L, et al. Magnetic iron oxide nanoparticles: synthesis, stabilization, vectorization, physicochemical characterizations, and biological applications. *Chem Rev*. 2008; 108: 2064-110.
80. Hasany S, Ahmed I, Rajan J, Rehman A. Systematic review of the preparation techniques of iron oxide magnetic nanoparticles. *Nanosci Nanotechnol*. 2012; 2: 148-58.
81. Sodipo BK, Aziz AA. Recent advances in synthesis and surface modification of superparamagnetic iron oxide nanoparticles with silica. *J Magn Magn Mater*. 2016; 416: 275-91.
82. Jabalera Y, Casares Atienza, Fernández Vivas, Peigneux A, Azuaga Fortes, Jimenez Lopez. Protein conservation method affects MamC-mediated biominerization of magnetic nanoparticles. *Cryst Growth Des*. 2019; 19: 1064-71.
83. Matsumoto Y, Chen R, Anikeeva P, Jasanoff A. Engineering intracellular biominerization and biosensing by a magnetic protein. *Nat Commun*. 2015; 6: 8721.
84. Wei H, Wang E. Fe_3O_4 magnetic nanoparticles as peroxidase mimetics and their applications in H_2O_2 and glucose detection. *Analytical Chemistry*. 2008; 80: 2250-4.
85. Zhang S, Zhao X, Niu H, Shi Y, Cai Y, Jiang G. Superparamagnetic Fe_3O_4 nanoparticles as catalysts for the catalytic oxidation of phenolic and aniline compounds. *J Hazard Mater*. 2009; 167: 560-6.
86. Song C, Sun W, Xiao Y, Shi X. Ultrasmall iron oxide nanoparticles: synthesis, surface modification, assembly, and biomedical applications. *Drug Discov Today*. 2019; 24: 835-44.
87. Hu Y, Mignani S, Majoral J-P, Shen M, Shi X. Construction of iron oxide nanoparticle-based hybrid platforms for tumor imaging and therapy. *Chem Soc Rev*. 2018; 47: 1874-900.
88. Park J, An K, Hwang Y, Park J, Noh H, Kim J, et al. Ultra-large-scale syntheses of monodisperse nanocrystals. *Nat Mater*. 2004; 3: 891-5.
89. Lu AH, Salabas Eel, Schüth F. Magnetic nanoparticles: synthesis, protection, functionalization, and application. *Angew Chem Int Ed Engl*. 2007; 46: 1222-44.
90. Deng H, Li X, Peng Q, Wang X, Chen J, Li Y. Monodisperse magnetic single-crystal ferrite microspheres. *Angewandte Chemie*. 2005; 117: 2842-5.
91. Fiévet F, Ammar Merah, Brayner R, et al. The polyol process: a unique method for easy access to metal nanoparticles with tailored sizes, shapes and compositions. *Chem Soc Rev*. 2018; 47: 5187-5233.
92. Li J, Zheng L, Cai H, Sun W, Shen M, Zhang G, et al. Polyethyleneimine-mediated synthesis of folic acid-targeted iron oxide nanoparticles for in vivo tumor MR imaging. *Biomaterials*. 2013; 34: 8382-92.
93. Frimpong RA, Dou J, Pecham M, Hilt JZ. Enhancing remote controlled heating characteristics in hydrophilic magnetite nanoparticles via facile co-precipitation. *J Magn Magn Mater*. 2010; 322: 326-31.
94. Massart R. Preparation of aqueous magnetic liquids in alkaline and acidic media. *IEEE Trans Magn*. 1981; 17: 1247-8.
95. Liang X, Wang X, Zhuang J, Chen Y, Wang D, Li Y. Synthesis of nearly monodisperse iron oxide and oxyhydroxide nanocrystals. *Adv Funct Mater*. 2006; 16: 1805-13.
96. Singh RK, Patel KD, Kim J-J, Kim T-H, Kim J-H, Shin US, et al. Multifunctional hybrid nanocarrier: magnetic CNTs ensheathed with mesoporous silica for drug delivery and imaging system. *ACS Appl Mater Interfaces*. 2014; 6: 2201-8.
97. Zhang L, Qiao S, Jin Y, Chen Z, Gu H, Lu GQ. Magnetic hollow spheres of periodic mesoporous organosilica and Fe_3O_4 nanocrystals: fabrication and structure control. *Adv Mater*. 2008; 20: 805-9.
98. Na HB, Song IC, Hyeon T. Inorganic nanoparticles for MRI contrast agents. *Adv Mater*. 2009; 21: 2133-48.
99. Talapin DV, Lee J-S, Kovalenko MV, Shevchenko EV. Prospects of colloidal nanocrystals for electronic and optoelectronic applications. *Chem Rev*. 2009; 110: 389-458.
100. Tartaj P, Del M, Veintemillas Verdaguera, González T, Serna CJ. The preparation of magnetic nanoparticles for applications in biomedicine. *J Phys D Appl Phys*. 2003; 36: 182-97.
101. Liang M, Lu J, Kovochich M, Xia T, Ruehm SG, Nel AE, et al. Multifunctional inorganic nanoparticles for imaging, targeting, and drug delivery. *ACS nano*. 2008; 2: 889-96.
102. Henderson L, Neumann O, Kaffes C, Zhang R, Marangoni V, Ravoori MK, et al. Routes to potentially safer T_1 magnetic resonance imaging contrast in a compact plasmonic nanoparticle with enhanced fluorescence. *ACS nano*. 2018; 12: 8214-23.
103. Zhong LS, Hu JS, Liang HP, Cao AM, Song WG, Wan LJ. Self-Assembled 3D flowerlike iron oxide nanostructures and their application in water treatment. *Adv Mater*. 2006; 18: 2426-31.
104. Zhao N, Yan L, Zhao X, Chen X, Li A, Zheng D, et al. Versatile types of organic/inorganic nanohybrids: from strategic design to biomedical applications. *Chem Rev*. 2018; 119: 1666-762.
105. Ferrucci J, Stark D. Iron oxide-enhanced MR imaging of the liver and spleen: review of the first 5 years. *AJR Am J Roentgenol*. 1990; 155: 943-50.
106. Cai W, Wan J. Facile synthesis of superparamagnetic magnetite nanoparticles in liquid polyols. *J Colloid Interface Sci*. 2007; 305: 366-70.
107. Cai H, An X, Cui J, Li J, Wen S, Li K, et al. Facile hydrothermal synthesis and surface functionalization of polyethyleneimine-coated iron oxide nanoparticles for biomedical applications. *ACS Appl Mater Interfaces*. 2013; 5: 1722-31.
108. Cai H, Li K, Li J, Wen S, Chen Q, Shen M, et al. Dendrimer - assisted formation of $\text{Fe}_3\text{O}_4/\text{Au}$ nanocomposite particles for targeted dual mode CT/MR imaging of tumors. *Small*. 2015; 11: 4584-93.
109. Kang YS, Risbud S, Rabolt JF, Stroewe P. Synthesis and characterization of nanometer-size Fe_3O_4 and $\gamma\text{-Fe}_2\text{O}_3$ particles. *Chemistry of Materials*. 1996; 8: 2209-11.
110. Bai F, Wang D, Huo Z, Chen W, Liu L, Liang X, et al. A versatile bottom-up assembly approach to colloidal spheres from nanocrystals. *Angew Chem Int Ed Engl*. 2007; 46: 6650-3.
111. Wang L, Li Y. Controlled synthesis and luminescence of lanthanide doped NaYF_4 nanocrystals. *Chemistry of Materials*. 2007; 19: 727-34.
112. Jia G, You H, Liu K, Zheng Y, Guo N, Zhang H. Highly uniform Gd_2O_3 hollow microspheres: template-directed synthesis and luminescence properties. *Langmuir*. 2009; 26: 5122-8.
113. Iram M, Guo C, Guan Y, Ishfaq A, Liu H. Adsorption and magnetic removal of neutral red dye from aqueous solution using Fe_3O_4 hollow nanospheres. *J Hazard Mater*. 2010; 181: 1039-50.
114. Yang Z, Niu Z, Lu Y, Hu Z, Han CC. Templated synthesis of inorganic hollow spheres with a tunable cavity size onto core-shell gel particles. *Angew Chem Int Ed Engl*. 2003; 42: 1943-5.
115. Hosein ID, Liddell CM. Homogeneous, core-shell, and hollow-shell ZnS colloid-based photonic crystals. *Langmuir*. 2007; 23: 2892-7.
116. Chen M, Wu L, Zhou S, You B. A method for the fabrication of monodisperse hollow silica spheres. *Adv Mater*. 2006; 18: 801-6.
117. Lee J, Yang J, Kwon SG, Hyeon T. Nonclassical nucleation and growth of inorganic nanoparticles. *Nat Rev Mater*. 2016; 1: 16034.
118. Kango S, Kalia S, Celli A, Njuguna J, Habibi Y, Kumar R. Surface modification of inorganic nanoparticles for development of organic-inorganic nanocomposites-A review. *Prog Colloid Polym Sci*. 2013; 38: 1232-61.
119. Grillo R, Rosa AH, Fraceto LF. Engineered nanoparticles and organic matter: a review of the state-of-the-art. *Chemosphere*. 2015; 119: 608-19.
120. Turcheniuk K, Tarasevych AV, Kukhar VP, Boukherroub R, Szunerits S. Recent advances in surface chemistry strategies for the fabrication of functional iron oxide based magnetic nanoparticles. *Nanoscale*. 2013; 5: 10729-52.
121. Gawande MB, Luque R, Zboril R. The rise of magnetically recyclable nanocatalysts. *ChemCatChem*. 2014; 6: 3312-3.
122. Liu B, Liu J. Surface modification of nanozymes. *Nano Research*. 2017; 10: 1125-48.
123. Valdiglesias V, Fernández-Bertólez N, Kılıç G, Costa C, Costa S, Fraga S, et al. Are iron oxide nanoparticles safe? Current knowledge and future perspectives. *Journal of Trace Elements in Medicine and Biology*. 2016; 38: 53-63.
124. Chakrabarty R, Hong H, Cai W. Positron emission tomography image-guided drug delivery: current status and future perspectives. *Mol Pharm*. 2014; 11: 3777-97.
125. Karimzadeh I, Aghazadeh M, Ganjali MR, Norouzi P, Doroudi T, Kolivand PH. Saccharide-coated superparamagnetic Fe_3O_4 nanoparticles (SPIONs) for biomedical applications: an efficient and scalable route for preparation and in situ surface coating through cathodic electrochemical deposition (CED). *Mater Lett*. 2017; 189: 290-4.
126. Lee N, Cho HR, Oh MH, Lee SH, Kim K, Kim BH, et al. Multifunctional $\text{Fe}_3\text{O}_4/\text{TaO}_x$ core/shell nanoparticles for simultaneous magnetic resonance imaging and X-ray computed tomography. *Journal of the American Chemical Society*. 2012; 134: 10309-12.
127. Smith BR, Gambhir SS. Nanomaterials for in vivo imaging. *Chem Rev*. 2017; 117: 901-86.
128. Liu J, Liu Y, Bu W, Bu J, Sun Y, Du J, et al. Ultrasensitive nanosensors based on upconversion nanoparticles for selective hypoxia imaging in vivo upon near-infrared excitation. *Journal of the American Chemical Society*. 2014; 136: 9701-9.
129. Zhu J, Lu Y, Li Y, Jiang J, Cheng L, Liu Z, et al. Synthesis of $\text{Au}-\text{Fe}_3\text{O}_4$ heterostructured nanoparticles for in vivo computed tomography and magnetic resonance dual model imaging. *Nanoscale*. 2014; 6: 199-202.
130. Hu Y, Wang R, Wang S, Ding L, Li J, Luo Y, et al. Multifunctional $\text{Fe}_3\text{O}_4@\text{Au}$ core/shell nanostars: a unique platform for multimode imaging and photothermal therapy of tumors. *Scientific reports*. 2016; 6: 28325.
131. Tuo Y, Liu G, Dong B, Zhou J, Wang A, Wang J, et al. Microbial synthesis of $\text{Pd}/\text{Fe}_3\text{O}_4$, $\text{Au}/\text{Fe}_3\text{O}_4$ and $\text{PdAu}/\text{Fe}_3\text{O}_4$ nanocomposites for catalytic reduction of nitroaromatic compounds. *Scientific reports*. 2015; 5: 13515.
132. Zhu J, Zhang B, Tian J, Wang J, Chong Y, Wang X, et al. Synthesis of heterodimer radionuclide nanoparticles for magnetic resonance and single-photon emission computed tomography dual-modality imaging. *Nanoscale*. 2015; 7: 3392-5.
133. Cao M, Wang P, Kou Y, Wang J, Liu J, Li Y, et al. Gadolinium (III)-chelated silica nanospheres integrating chemotherapy and photothermal therapy for cancer treatment and magnetic resonance imaging. *ACS Appl Mater Interfaces*. 2015; 7: 25014-23.
134. Qu X, Yang F, Chen H, Li J, Zhang H, Zhang G, et al. Bubble-mediated ultrasensitive multiplex detection of metal ions in three-dimensional DNA

- nanostructure-encoded microchannels. *ACS Appl Mater Interfaces.* 2017; 9: 16026-34.
135. Bastakoti BP, Hsu YC, Liao SH, Wu KCW, Inoue M, Yusa Si, et al. Inorganic-organic hybrid nanoparticles with biocompatible calcium phosphate thin shells for fluorescence enhancement. *Chem Asian J.* 2013; 8: 1301-5.
136. Colombo M, Carregal S, Casula MF, Gutiérrez L, Morales MP, Böhm IB, et al. Biological applications of magnetic nanoparticles. *Chem Soc Rev.* 2012; 41: 4306-34.
137. Tian X, Zhang L, Yang M, Bai L, Dai Y, Yu Z, et al. Functional magnetic hybrid nanomaterials for biomedical diagnosis and treatment. *Wiley Interdiscip Rev Nanomed Nanobiotechnol.* 2018; 10: e1476.
138. Mura S, Nicolas J, Couvreur P. Stimuli-responsive nanocarriers for drug delivery. *Nat Mater.* 2013; 12: 991-1003.
139. Banchelli M, Nappini S, Montis C, Bonini M, Canton P, Berti D, et al. Magnetic nanoparticle clusters as actuators of ssDNA release. *Physical Chemistry Chemical Physics.* 2014; 16: 10023-31.
140. Ruiz-Hernandez E, Baeza A, Vallet-Regí M. Smart drug delivery through DNA/magnetic nanoparticle gates. *ACS nano.* 2011; 5: 1259-66.
141. Li F, Lu J, Kong X, Hyeon T, Ling D. Dynamic nanoparticle assemblies for biomedical applications. *Adv Mater.* 2017; 29: 1605897.
142. Sun W, Mignani S, Shen M, Shi X. Dendrimer-based magnetic iron oxide nanoparticles: their synthesis and biomedical applications. *Drug Discov Today.* 2016; 21: 1873-85.
143. Geng H, Zhou Q, Zheng J, Gu H. Preparation of porous and hollow Fe₃O₄@C spheres as an efficient anode material for a high-performance Li-ion battery. *RSC Adv.* 2014; 4: 6430-4.
144. Majeed J, Pradhan L, Ningthoujam RS, Vatsa RK, Bahadur D, Tyagi AK. Enhanced specific absorption rate in silanol functionalized Fe₃O₄ core-shell nanoparticles: Study of Fe leaching in Fe₃O₄ and hyperthermia in L929 and HeLa cells. *Colloids Surf B Biointerfaces.* 2014; 122: 396-403.
145. Dong Z, Feng L, Hao Y, Chen M, Gao M, Chao Y, et al. Synthesis of hollow biomimetic CaCO₃-polydopamine nanoparticles for multimodal imaging-guided cancer photodynamic therapy with reduced skin photosensitivity. *Journal of the American Chemical Society.* 2018; 140: 2165-78.
146. Schmid G. Nanoparticles: from theory to application: John Wiley & Sons; 2011.
147. Tang F, Li L, Chen D. Mesoporous silica nanoparticles: synthesis, biocompatibility and drug delivery. *Adv Mater.* 2012; 24: 1504-34.
148. Neamtu M, Nadejde C, Hodoroaba VD, Schneider RJ, Verestuci L, Panne U. Functionalized magnetic nanoparticles: Synthesis, characterization, catalytic application and assessment of toxicity. *Scientific reports.* 2018; 8: 6278.
149. Yang P, Gai S, Lin J. Functionalized mesoporous silica materials for controlled drug delivery. *Chem Soc Rev.* 2012; 41: 3679-98.
150. Xia T, Kovochich M, Liong M, Meng H, Kabehie S, George S, et al. Polyethyleneimine coating enhances the cellular uptake of mesoporous silica nanoparticles and allows safe delivery of siRNA and DNA constructs. *ACS nano.* 2009; 3: 3273-86.
151. Lin Y, Haynes CL. Impacts of mesoporous silica nanoparticle size, pore ordering, and pore integrity on hemolytic activity. *Journal of the American Chemical Society.* 2010; 132: 4834-42.
152. Lee JE, Lee N, Kim T, Kim J, Hyeon T. Multifunctional mesoporous silica nanocomposite nanoparticles for theranostic applications. *Acc Chem Res.* 2011; 44: 893-902.
153. Kim J, Kim HS, Lee N, Kim T, Kim H, Yu T, et al. Multifunctional uniform nanoparticles composed of a magnetite nanocrystal core and a mesoporous silica shell for magnetic resonance and fluorescence imaging and for drug delivery. *Angew Chem Int Ed Engl.* 2008; 47: 8438-41.
154. Lin L, Cong Z, Cao J, Ke K, Peng Q, Gao J, et al. Multifunctional Fe₃O₄@ polydopamine core-shell nanocomposites for intracellular mRNA detection and imaging-guided photothermal therapy. *ACS nano.* 2014; 8: 3876-83.
155. Jun Y, Seo J, Cheon J. Nanoscaling laws of magnetic nanoparticles and their applicabilities in biomedical sciences. *Acc Chem Res.* 2008; 41: 179-89.
156. Jiang J, Gu H, Shao H, Devlin E, Papaefthymiou GC, Ying JY. Bifunctional Fe₃O₄-Ag heterodimer nanoparticles for two-photon fluorescence imaging and magnetic manipulation. *Adv Mater.* 2008; 20: 4403-7.
157. Li J, Hu Y, Yang J, Wei P, Sun W, Shen M, et al. Hyaluronic acid-modified Fe₃O₄@Au core/shell nanostars for multimodal imaging and photothermal therapy of tumors. *Biomaterials.* 2015; 38: 10-21.
158. Dong W, Li Y, Niu D, Ma Z, Gu J, Chen Y, et al. Facile synthesis of monodisperse superparamagnetic Fe₃O₄ core@hybrid@Au shell nanocomposite for bimodal imaging and photothermal therapy. *Adv Mater.* 2011; 23: 5392-7.
159. Das R, Rinaldi-Montes N, Alonso J, Amghous Z, Garaio E, García J, et al. Boosted hyperthermia therapy by combined AC magnetic and photothermal exposures in Ag/Fe₃O₄ nanoflowers. *ACS Appl Mater Interfaces.* 2016; 8: 25162-9.
160. Lu S, Li X, Zhang J, Peng C, Shen M, Shi X. Dendrimer-stabilized gold nanoflowers embedded with ultrasmall iron oxide nanoparticles for multimode imaging-guided combination therapy of tumors. *Adv Sci.* 2018; 5: 1801612.
161. Shi J, Kantoff PW, Wooster R, Farokhzad OC. Cancer nanomedicine: progress, challenges and opportunities. *Nat Rev Cancer.* 2017; 17: 20-37.
162. Guerrero Martinez, Pérez Juste, Liz Marzán. Recent progress on silica coating of nanoparticles and related nanomaterials. *Adv Mater.* 2010; 22: 1182-95.
163. Xuan S, Wang Y, Leung KC, Shu K. Synthesis of Fe₃O₄@polyaniline core/shell microspheres with well-defined blackberry-like morphology. *The Journal of Physical Chemistry C.* 2008; 112: 18804-9.
164. Wang X, Tu Q, Zhao B, An Y, Wang J, Liu W, et al. Effects of poly (L-lysine)-modified Fe₃O₄ nanoparticles on endogenous reactive oxygen species in cancer stem cells. *Biomaterials.* 2013; 34: 1155-69.
165. Wang Y, Teng X, Wang J-S, Yang H. Solvent-free atom transfer radical polymerization in the synthesis of Fe₃O₄@polystyrene core-shell nanoparticles. *Nano Lett.* 2003; 3: 789-93.
166. Rajan M, Raj V. Potential drug delivery applications of chitosan based nanomaterials. *Int J Eng Res Appl.* 2013; 5: 145-55.
167. Hadjidemetriou M, Ahmadz Z, Mazza M, Collins RF, Dawson K, Kostarelos K. In vivo biomolecule corona around blood-circulating, clinically used and antibody-targeted lipid bilayer nanoscale vesicles. *ACS nano.* 2015; 9: 8142-56.
168. Pasut G, Paolino D, Celia C, Mero A, Joseph AS, Wolfram J, et al. Polyethylene glycol (PEG)-dendron phospholipids as innovative constructs for the preparation of super stealth liposomes for anticancer therapy. *J Control Release.* 2015; 199: 106-13.
169. Dehaini D, Fang RH, Luk BT, Pang Z, Hu C-MJ, Kroll AV, et al. Ultra-small lipid-polymer hybrid nanoparticles for tumor-penetrating drug delivery. *Nanoscale.* 2016; 8: 14411-9.
170. Xu S, Yang F, Zhou X, Zhuang Y, Liu B, Mu Y, et al. Uniform PEGylated PLGA microcapsules with embedded Fe₃O₄ nanoparticles for US/MR dual-modality imaging. *ACS Appl Mater Interfaces.* 2015; 7: 20460-8.
171. Gu Z, Chen L, Duan B, Luo Q, Liu J, Duan C. Synthesis of Au@UiO-66 (NH) structures by small molecule-assisted nucleation for plasmon-enhanced photocatalytic activity. *Chem Commun.* 2016; 52: 116-9.
172. Lin J, Xin P, An L, Xu Y, Tao C, Tian Q, et al. Fe₃O₄-ZIF-8 assemblies as pH and glutathione responsive T₂-T₁ switching magnetic resonance imaging contrast agent for sensitive tumor imaging in vivo. *Chem Commun.* 2019; 55: 478-81.
173. Fang C, Deng Z, Cao G, Chu Q, Wu Y, Li X, et al. Co-Ferroocene MOF/Glucose Oxidase as Cascade Nanozyme for Effective Tumor Therapy. *Adv Funct Mater.* 2020; 1910085.
174. Agasti SS, Rana S, Park MH, Kim CK, You CC, Rotello VM. Nanoparticles for detection and diagnosis. *Adv Drug Deliv Rev.* 2010; 62: 316-28.
175. Saha K, Agasti SS, Kim C, Li X, Rotello VM. Gold nanoparticles in chemical and biological sensing. *Chem Rev.* 2012; 112: 2739-79.
176. Iversen TG, Skotland T, Sandvig K. Endocytosis and intracellular transport of nanoparticles: present knowledge and need for future studies. *Nano today.* 2011; 6: 176-85.
177. Mattoussi H, Palui G, Na HB. Luminescent quantum dots as platforms for probing in vitro and in vivo biological processes. *Adv Drug Deliv Rev.* 2012; 64: 138-66.
178. Zolnik BS, Gonzalez-Fernandez A, Sadrieh N, Dobrovolskaia MA. Minireview: nanoparticles and the immune system. *Endocrinology.* 2010; 151: 458-65.
179. Lu Y, Aimetti AA, Langer R, Gu Z. Bioreponsive materials. *Nat Rev Mater.* 2017; 2: 16075.
180. Zhou Z, Song J, Nie L, Chen X. Reactive oxygen species generating systems meeting challenges of photodynamic cancer therapy. *Chem Soc Rev.* 2016; 45: 6597-626.
181. Hu C, Zhang L, Aryal S, Cheung C, Fang RH, Zhang L. Erythrocyte membrane-camouflaged polymeric nanoparticles as a biomimetic delivery platform. *Proceedings of the National Academy of Sciences.* 2011; 108: 10980-5.
182. Yao C, Wang W, Wang P, Zhao M, Li X, Zhang F. Near-infrared upconversion mesoporous cerium oxide hollow biophotocatalyst for concurrent pH-/H₂O₂-responsive O²⁻ evolving synergistic cancer therapy. *Adv Mater.* 2018; 30: 1704833.
183. Rao L, Bu LL, Meng QF, Cai B, Deng WW, Li A, et al. Antitumor platelet-mimicking magnetic nanoparticles. *Adv Funct Mater.* 2017; 27: 1604774.
184. Kratz H, Taupitz M, de Schellenberger AA, Kosch O, Eberbeck D, Wagner S, et al. Novel magnetic multicore nanoparticles designed for MPI and other biomedical applications: From synthesis to first in vivo studies. *PLoS One.* 2018; 13: e0190214.
185. Yang F, Zhang M, He W, Chen P, Cai X, Yang L, et al. Controlled release of Fe₃O₄ nanoparticles in encapsulated microbubbles to tumor cells via sonoporation and associated cellular bioeffects. *Small.* 2011; 7: 902-10.
186. Li C, Chen T, Ocsoy I, Zhu G, Yasun E, You M, et al. Gold-coated Fe₃O₄ nanoroses with five unique functions for cancer cell targeting, imaging, and therapy. *Adv Funct Mater.* 2014; 24: 1772-80.
187. Miao Q, Pu K. Organic semiconducting agents for deep-tissue molecular imaging: second near-infrared fluorescence, self-luminescence, and photoacoustics. *Adv Mater.* 2018; 30: 1801778.
188. Sun W, Yang J, Zhu J, Zhou Y, Li J, Zhu X, et al. Immobilization of iron oxide nanoparticles within alginate nanogels for enhanced MR imaging applications. *Biomater Sci.* 2016; 4: 1422-30.
189. Kim BH, Lee N, Kim H, An K, Park YI, Choi Y, et al. Large-scale synthesis of uniform and extremely small-sized iron oxide nanoparticles for high-resolution T₁ magnetic resonance imaging contrast agents. *Journal of the American Chemical Society.* 2011; 133: 12624-31.
190. Lee N, Kim H, Choi SH, Park M, Kim D, Kim HC, et al. Magnetosome-like ferrimagnetic iron oxide nanocubes for highly sensitive MRI of single cells and transplanted pancreatic islets. *Proceedings of the National Academy of Sciences.* 2011; 108: 2662-7.

191. Ma D, Chen J, Luo Y, Wang H, Shi X. Zwitterion-coated ultrasmall iron oxide nanoparticles for enhanced T₁-weighted magnetic resonance imaging applications. *J Mater Chem B*. 2017; 5: 7267-73.
192. Wu W, Jiang C, Roy VA. Recent progress in magnetic iron oxide-semiconductor composite nanomaterials as promising photocatalysts. *Nanoscale*. 2015; 7: 38-58.
193. Wei H, Bruns OT, Kaul MG, Hansen EC, Barch M, Wiśniowska A, et al. Exceedingly small iron oxide nanoparticles as positive MRI contrast agents. *Proceedings of the national academy of sciences*. 2017; 114: 2325-30.
194. Peng Y, Liu C, Chen H, Chou S, Tseng W, Tseng Y, et al. Antiferromagnetic iron nanocolloids: A new generation *in vivo* T₁ MRI contrast agent. *Journal of the American Chemical Society*. 2013; 135: 18621-8.
195. Lu Y, Xu Y, Zhang G, Ling D, Wang M, Zhou Y, et al. Iron oxide nanoclusters for T₁ magnetic resonance imaging of non-human primates. *Nat Biomed Eng*. 2017; 1: 637-43.
196. Sherwood J, Rich M, Lovas K, Warram J, Bolding M, Bao Y. T₁-Enhanced MRI-visible nanoclusters for imaging-guided drug delivery. *Nanoscale*. 2017; 9: 11785-92.
197. Wang L, Huang J, Chen H, Wu H, Xu Y, Li Y, et al. Exerting enhanced permeability and retention effect driven delivery by ultrafine iron oxide nanoparticles with T₁-T₂ switchable magnetic resonance imaging contrast. *Acad Nano*. 2017; 11: 4582-92.
198. Tian Q, Hu J, Zhu Y, Zou R, Chen Z, Yang S, et al. Sub-10 nm Fe₃O₄@Cu_{2-x}S core-shell nanoparticles for dual-modal imaging and photothermal therapy. *Journal of the American Chemical Society*. 2013; 135: 8571-7.
199. Im GH, Kim SM, Lee DG, Lee WJ, Lee JH, Lee IS. Fe₃O₄/MnO hybrid nanocrystals as a dual contrast agent for both T₁-and T₂-weighted liver MRI. *Biomaterials*. 2013; 34: 2069-76.
200. Feng L, Yang D, He F, Gai S, Li C, Dai Y, et al. A Core-Shell-Satellite Structured Fe₃O₄@g-C₃N₄-UCNPs-PEG for T₁/T₂-Weighted Dual-Modal MRI-Guided Photodynamic Therapy. *Adv Healthc Mater*. 2017; 6: 1700502.
201. Gao L, Zhuang J, Nie L, Zhang J, Zhang Y, Gu N, et al. Intrinsic peroxidase-like activity of ferromagnetic nanoparticles. *Nat Nanotechnol*. 2007; 2: 577-83.
202. Gao L, Fan K, Yan X. Iron oxide nanozyme: a multifunctional enzyme mimetic for biomedical applications. *Theranostics*. 2017; 7: 3207-27.
203. Shen Z, Song J, Yung BC, Zhou Z, Wu A, Chen X. Emerging strategies of cancer therapy based on ferroptosis. *Adv Mater*. 2018; 30: 1704007.
204. Brillas E, Sirés I, Oturan MA. Electro-Fenton process and related electrochemical technologies based on Fenton's reaction chemistry. *Chem Rev*. 2009; 109: 6570-631.
205. Bokare AD, Choi W. Review of iron-free Fenton-like systems for activating H₂O₂ in advanced oxidation processes. *J Hazard Mater*. 2014; 275: 121-35.
206. Shen Z, Liu T, Li Y, Lau J, Yang Z, Fan W, et al. Fenton-reaction-accelerable magnetic nanoparticles for ferroptosis therapy of orthotopic brain tumors. *ACS nano*. 2018; 12: 11355-65.
207. Bi H, Dai Y, Yang P, Xu J, Yang D, Gai S, et al. Glutathione mediated size-tunable UCNPs-Pt (IV)-ZnFe₂O₄ nanocomposite for multiple bioimaging guided synergistic therapy. *Small*. 2018; 14: 1703809.
208. Mijangos F, Varona F, Villota N. Changes in solution color during phenol oxidation by Fenton reagent. *Environ Sci Technol*. 2006; 40: 5538-43.
209. Wang X, Xu J, Yang D, Sun C, Sun Q, He F, et al. Fe₃O₄@MIL-100(Fe)-UCNPs heterojunction photosensitizer: Rational design and application in near infrared light mediated hypoxic tumor therapy. *Chem Eng J*. 2018; 354: 1141-52.
210. Chen Z, Yin J, Zhou Y, Zhang Y, Song L, Song M, et al. Dual enzyme-like activities of iron oxide nanoparticles and their implication for diminishing cytotoxicity. *ACS Nano*. 2012; 6: 4001-12.
211. Zhao Y, Ding B, Xiao X, Jiang F, Wang M, Hou Z, et al. Virus-Like Fe₃O₄@Bi₂S₃ Nanozymes with Resistance Free Apoptotic Hyperthermia-Augmented Nanozymitic Activity for Enhanced Synergetic Cancer Therapy. *ACS Appl Mater Interfaces*. 2020; 12: 11320-8.
212. Guardia P, Di Corato R, Lartigue L, Wilhelm C, Espinosa A, Garcia-Hernandez M, et al. Water-soluble iron oxide nanocubes with high values of specific absorption rate for cancer cell hyperthermia treatment. *ACS nano*. 2012; 6: 3080-91.
213. Lartigue L, Innocenti C, Kalaivani T, Awwad A, Sanchez Duque MdM, Guar Y, et al. Water-dispersible sugar-coated iron oxide nanoparticles. An evaluation of their relaxometric and magnetic hyperthermia properties. *Journal of the American Chemical Society*. 2011; 133: 10459-72.
214. Hayashi K, Nakamura M, Sakamoto W, Yogo T, Miki H, Ozaki S, et al. Superparamagnetic nanoparticle clusters for cancer theranostics combining magnetic resonance imaging and hyperthermia treatment. *Theranostics*. 2013; 3: 366-76.
215. Ma X, Wang Y, Liu X, Ma H, Li G, Li Y, et al. Fe₃O₄-Pd Janus nanoparticles with amplified dual-mode hyperthermia and enhanced ROS generation for breast cancer treatment. *Nanoscale Horiz*. 2019; 4: 1450-9.
216. Yang G, Gong H, Liu T, Sun X, Cheng L, Liu Z. Two-dimensional magnetic WS₂@Fe₃O₄ nanocomposite with mesoporous silica coating for drug delivery and imaging-guided therapy of cancer. *Biomaterials*. 2015; 60: 62-71.
217. Shen S, Tang H, Zhang X, Ren J, Pang Z, Wang D, et al. Targeting mesoporous silica-encapsulated gold nanorods for chemo-photothermal therapy with near-infrared radiation. *Biomaterials*. 2013; 34: 3150-8.
218. Du Y, Liu W, Qiang R, Wang Y, Han X, Ma J, et al. Shell thickness-dependent microwave absorption of core-shell Fe₃O₄@C composites. *ACS Appl Mater Interfaces*. 2014; 6: 12997-3006.
219. Tsai M, Chang S-HG, Cheng F, Shanmugam V, Cheng Y, Su C, et al. Au nanorod design as light-absorber in the first and second biological near-infrared windows for *in vivo* photothermal therapy. *ACS nano*. 2013; 7: 5330-42.
220. Bagley AF, Hill S, Rogers GS, Bhatia SN. Plasmonic photothermal heating of intraperitoneal tumors through the use of an implanted near-infrared source. *ACS nano*. 2013; 7: 8089-97.
221. Shen S, Wang S, Zheng R, Zhu X, Jiang X, Fu D, et al. Magnetic nanoparticle clusters for photothermal therapy with near-infrared irradiation. *Biomaterials*. 2015; 39: 67-74.
222. Lin K, Cao Y, Zheng D, Li Q, Liu H, Yu P, et al. Facile phase transfer of hydrophobic Fe₃O₄@Cu_{2-x}S nanoparticles by red blood cell membrane for MRI and phototherapy in the second near-infrared window. *J Mater Chem B*. 2020; 8: 1202-11.
223. Zhou Z, Sun Y, Shen J, Wei J, Yu C, Kong B, et al. Iron/iron oxide core/shell nanoparticles for magnetic targeting MRI and near-infrared photothermal therapy. *Biomaterials*. 2014; 35: 7470-8.
224. Chu M, Shao Y, Peng J, Dai X, Li H, Wu Q, et al. Near-infrared laser light mediated cancer therapy by photothermal effect of Fe₃O₄ magnetic nanoparticles. *Biomaterials*. 2013; 34: 4078-88.
225. Zhang X, Xu X, Li T, Lin M, Lin X, Zhang H, et al. Composite photothermal platform of polypyrrrole-enveloped Fe₃O₄ nanoparticle self-assembled superstructures. *ACS Appl Mater Interfaces*. 2014; 6: 14552-61.
226. Dormer K, Awasthi V, Galbraith W, Kopke R, Chen K, Wassel R. Magnetically-targeted, technetium 99m-labeled nanoparticles to the inner ear. *Journal of Biomedical Nanotechnology*. 2008; 4: 174-84.
227. Ge R, Liu C, Zhang X, Wang W, Li B, Liu J, et al. Photothermal-activatable Fe₃O₄ superparticle nanodrug carriers with PD-L1 immune checkpoint blockade for anti-metastatic cancer immunotherapy. *ACS Appl Mater Interfaces*. 2018; 10: 20342-55.
228. Liu B, Li C, Chen G, Liu B, Deng X, Wei Y, et al. Synthesis and optimization of MoS₂@Fe₃O₄:ICG/Pt (IV) nanoflowers for MR/IR/PA bioimaging and combined PTT/PDT/chemotherapy triggered by 808 nm laser. *Adv Sci*. 2017; 4: 1600540.
229. Yang Y, Wang C, Tian C, Guo H, Shen Y, Zhu M. Fe₃O₄@MnO₂@PPy nanocomposites overcome hypoxia: magnetic-targeting-assisted controlled chemotherapy and enhanced photodynamic/photothermal therapy. *J Mater Chem B*. 2018; 6: 6848-57.
230. Weir BA, Woo MS, Getz G, Perner S, Ding L, Beroukhim R, et al. Characterizing the cancer genome in lung adenocarcinoma. *Nature*. 2007; 450: 893-98.
231. Workman P, Aboagye E, Balkwill F, Balmain A, Bruder G, Chaplin D, et al. Guidelines for the welfare and use of animals in cancer research. *Br J Cancer*. 2010; 102: 1555-77.
232. Stratton MR, Campbell PJ, Futreal PA. The cancer genome. *Nature*. 2009; 458: 719-724.
233. Green ED, Guyer MS, Institute NHGR. Charting a course for genomic medicine from base pairs to bedside. *Nature*. 2011; 470: 204-13.
234. Hrkach J, Von Hoff D, Ali MM, Andrianova E, Auer J, Campbell T, et al. Preclinical development and clinical translation of a PSMA-targeted docetaxel nanoparticle with a differentiated pharmacological profile. *Science translational medicine*. 2012; 4: 128.
235. Gluz O, Liedtke C, Gottschalk N, Pusztai L, Nitz U, Harbeck N. Triple-negative breast cancer-current status and future directions. *Annals of Oncology*. 2009; 20: 1913-27.
236. Ruoslahti E, Bhatia SN, Sailor MJ. Targeting of drugs and nanoparticles to tumors. *The Journal of cell biology*. 2010; 188: 759-68.
237. Schroeder A, Heller DA, Winslow MM, Dahlman JE, Pratt GW, Langer R, et al. Treating metastatic cancer with nanotechnology. *Nat Rev Cancer*. 2012; 12: 39-50.
238. Li S, Cheng H, Xie B, Qiu W, Zeng J, Li C, et al. Cancer cell membrane camouflaged cascade bioreactor for cancer targeted starvation and photodynamic therapy. *ACS nano*. 2017; 11: 7006-18.
239. Fang RH, Jiang Y, Jiang Y, Zhang L. Cell membrane-derived nanomaterials for biomedical applications. *Biomaterials*. 2017; 128: 69-83.
240. Liu J, Liang H, Li M, Luo Z, Zhang J, Guo X, et al. Tumor acidity activating multifunctional nanoplatform for NIR-mediated multiple enhanced photodynamic and photothermal tumor therapy. *Biomaterials*. 2018; 157: 107-24.
241. Lv Y, Liu M, Zhang Y, Wang X, Zhang F, Li F, et al. Cancer cell membrane-biomimetic nanoprobes with two-photon excitation and near-infrared emission for intravital tumor fluorescence imaging. *ACS nano*. 2018; 12: 1350-8.
242. Reguera J, de Aberasturi DJ, Henriksen-Lacey M, Langer J, Espinosa A, Szczupak B, et al. Janus plasmonic-magnetic gold-iron oxide nanoparticles as contrast agents for multimodal imaging. *Nanoscale*. 2017; 9: 9467-80.
243. Zhu X, Li J, Peng P, Hosseini Nassab N, Smith BR. Quantitative drug release monitoring in tumors of living subjects by magnetic particle imaging nanocomposite. *Nano Lett*. 2019; 19: 6725-33.
244. Wang X, Hu Y, Wei H. Nanozymes in bionanotechnology: from sensing to therapeutics and beyond. *Inorg Chem Front*. 2016; 3: 41-60.

245. Kim J, Lee JE, Lee SH, Yu JH, Lee JH, Park TG, et al. Designed fabrication of a multifunctional polymer nanomedical platform for simultaneous cancer-targeted imaging and magnetically guided drug delivery. *Adv Mater.* 2008; 20: 478-83.
246. Fang RH, Kroll AV, Gao W, Zhang L. Cell membrane coating nanotechnology. *Adv Mater.* 2018; 30: 1706759.
247. Ceccaldi R, Liu JC, Amunugama R, Hajdu I, Primack B, Petalcorin MI, et al. Homologous-recombination-deficient tumours are dependent on Pol β -mediated repair. *Nature.* 2015; 518: 258.
248. Chen Z, Zhao P, Luo Z, Zheng M, Tian H, Gong P, et al. Cancer cell membrane-biomimetic nanoparticles for homologous-targeting dual-modal imaging and photothermal therapy. *ACS nano.* 2016; 10: 10049-57.
249. Konstantinopoulos PA, Ceccaldi R, Shapiro GI, D'Andrea AD. Homologous recombination deficiency: exploiting the fundamental vulnerability of ovarian cancer. *Cancer discovery.* 2015; 5: 1137-54.
250. Zhu J, Zheng D, Zhang M, Yu W, Qiu W, Hu J, et al. Preferential cancer cell self-recognition and tumor self-targeting by coating nanoparticles with homotypic cancer cell membranes. *Nano Lett.* 2016; 16: 5895-901.
251. Shen J, Xu R, Mai J, Kim H-C, Guo X, Qin G, et al. High capacity nanoporous silicon carrier for systemic delivery of gene silencing therapeutics. *ACS nano.* 2013; 7: 9867-80.
252. Shen J, Kim HC, Mu C, Gentile E, Mai J, Wolfram J, et al. Multifunctional gold nanorods for siRNA gene silencing and photothermal therapy. *Adv Healthc Mater.* 2014; 3: 1629-37.
253. Shen J, Wu X, Lee Y, Wolfram J, Yang Z, Mao Z, et al. Porous silicon microparticles for delivery of siRNA therapeutics. *J Vis Exp.* 2015; e52075.
254. Shen J, Wolfram J, Ferrari M, Shen H. Taking the vehicle out of drug delivery. *Mater Today (Kidlington).* 2017; 20: 95-7.
255. Shen J, Kim HC, Wolfram J, Mu C, Zhang W, Liu H, et al. A liposome encapsulated ruthenium polypyridine complex as a theranostic platform for triple-negative breast cancer. *Nano Lett.* 2017; 17: 2913-20.
256. Shen J, Liu H, Mu C, Wolfram J, Zhang W, Kim HC, et al. Multi-step encapsulation of chemotherapy and gene silencing agents in functionalized mesoporous silica nanoparticles. *Nanoscale.* 2017; 9: 5329-41.
257. Shen J, Kim HC, Su H, Wang F, Wolfram J, Kirui D, et al. Cyclodextrin and polyethylenimine functionalized mesoporous silica nanoparticles for delivery of siRNA cancer therapeutics. *Theranostics.* 2014; 4: 487-97.
258. Xu R, Zhang G, Mai J, Deng X, Segura V, Wu S, et al. An injectable nanoparticle generator enhances delivery of cancer therapeutics. *Nat Biotechnol.* 2016; 34: 414-8.
259. Wang X, Zhou Z, Wang Z, Xue Y, Zeng Y, Gao J, et al. Gadolinium embedded iron oxide nanoclusters as T₁-T₂ dual-modal MRI-visible vectors for safe and efficient siRNA delivery. *Nanoscale.* 2013; 5: 8098-104.
260. Park K. The beginning of the end of the nanomedicine hype. *J Control Release.* 2019; 305: 221-2.

Author biography



Shengzhe Zhao received his B.S in Materials Physics from Nanjing University of Information Science & Technology in 2015, M.S. in Applied Chemistry from Jilin Agricultural University in 2018, then appointed as a research assistant at University of Chinese Academy of Sciences in 2018. Currently, he is a visiting scholar in School of Chemistry and Chemical Engineering in Shanghai Jiao Tong University. His research interest is theranostic multifunctional nanomaterials.



Xujiang Yu obtained his B.S. in Chemistry in 2011 and M.S. in Inorganic Chemistry in 2013 from Sun Yat-Sen University under the supervision of Prof. Zongwan Mao. Then he moved to Shanghai Jiao Tong University and received his PhD in Materials Science and Engineering in 2018, supervised by Prof. Wanwan Li. He is currently a postdoctoral fellow in School of Chemistry and Chemical Engineering in Shanghai Jiao Tong University. His research focuses on the engineering of multifunctional nanomaterials and nano-assemblies for biomedical applications, especially in cancer imaging and therapy.



Yuna Qian received her Ph.D degree in 2017 from Chongqing University. Now she is an assistant professor of Wenzhou Institute, University of Chinese Academy of Sciences. Her current research interests are mainly in nanomaterials for tumour microenvironment and inflammatory cells.



Wei Chen is a full professor of Ophthalmology and the Head of Cornea Service in the affiliated eye hospital of Wenzhou Medical University in Zhejiang Province and Director of Eye Clinic in Boao Super Hospital in Hainan province. He graduated from Wenzhou Medical University with Medical Degree in 1998 and Shanghai Fudan university with PhD in 2002. He was trained as postdoctoral research fellow in Schepens Eye Research Institute, an affiliate of Harvard Medical College and Ocular Surface Center in Baylor. He was

advisory member of China cornea society and founding member of Asia Dry Eye Society. His clinical and research interests include molecular mechanism and animal model of dry eye, corneal tissue engineering, corneal transplantation.



Jianliang Shen received his B.S in Applied Chemistry from Hunan University of Science and Technology in 2007, M.S. in Inorganic Chemistry from Xiangtan University in 2010, and Ph.D. degree in Inorganic Chemistry under supervision of Prof. Zong-Wan Mao at Sun Yat-Sen University in 2014, then started as a postdoctoral fellow under supervision of Prof. Haifa Shen in Houston Methodist Research Institute. He was appointed as a full professor at Wenzhou Medical University and University of Chinese Academy of Sciences in 2017. His research interests in novel hybrid nano/micro-particles for biomedical applications.